Université de Montréal

Predictive Carboplatin Treatment Response Models for Epithelial Ovarian Cancer: Comparison of 2D, 3D and in-vivo models

Par

Melica Nourmoussavi Brodeur

Faculté de médecine, Université de Montréal

Mémoire présenté en vue de l'obtention du grade de maîtrise en sciences (M. Sc.)

en Sciences Biomédicales, option Médecine Expérimentale

Décembre 2020

Université de Montréal

Factulté de Médecine, Université de Montréal

Ce mémoire intitulé

Predictive Carboplatin Treatment Response Models for Epithelial Ovarian Cancer: Comparison of 2D, 3D and in-vivo models

Présenté par

Melica Nourmoussavi Brodeur

A été évalué(e) par un jury composé des personnes suivantes

Saima Hassan

Président-rapporteur

Anne-Marie Mes-Masson

Directeur de recherche

Luke McCaffrey

Membre du jury

Résumé

L'adénocarcinome épithélial de l'ovaire (CEO) est le cancer gynécologique le plus mortel. La recherche de nouvelles thérapies repose principalement sur des modèles précliniques 2D et *in vivo* avec des lignées cellulaires (LC) pour générer les évidences nécessaires à l'initiation d'essais cliniques. Ce processus requiert des fonds substantiels en recherche/santé qui est associé à un taux d'attrition élevé laissant supposer des lacunes dans le modèle actuel. Nos publications antérieures suggèrent que la sensibilité *in vitro* de nos LC du CEO à la chimiothérapie carboplatin varie en 2D ou 3D. Il reste à élucider lequel de ces modèles est le plus représentatif de la réponse *in vivo*. De ce fait, nous avons émis l'hypothèse que le modèle 3D refléterait plus étroitement la sensibilité *in vivo*. L'objectif de cette étude était de caractériser la réponse au carboplatin de nos LC du CEO en monocouches et en sphéroïdes (3D), puis de les comparer à leur réponse *in vivo* (xénogreffes). Un total de 6 LC du CEO a été injecté dans des souris qui ont reçues trois différentes concentrations de carboplatin. Leurs réponses ont été évaluées/classées selon leurs mesures de volume tumoral et l'immunofluorescence. Ces mêmes LC ont été ensemencées dans des plaques à très faible adhérence pour former des sphéroïdes et les traiter. Des analyses de cytométrie en flux ont été effectuées afin de classer les LC selon leur concentration inhibitrice médiane (CI_{50}). Nous avons comparé le tout aux résultats 2D (CI_{50}) précédemment publiés. Nos résultats montrent que le système 3D démontre la meilleure concordance avec le modèle *in vivo*. Notamment, notre LC ultra-résistance en 2D devient plus sensible en modèle murin ou encore en 3D. Inversement, une LC ultra-sensible en 2D est plus résistante en xénogreffe et en sphéroïde. Les résultats découlant de notre étude sont importants à considérer lors d'investissement de temps et de fonds dans les études de criblage et de prédiction de réponses thérapeutiques.

Mots-clés : modèles précliniques, cancer de l'ovaire, xénogreffes, sphéroïdes, carboplatin

Abstract

Epithelial ovarian adenocarcinoma (EOC) is the most lethal gynecological cancer. The drug discovery pipeline is heavily based on preclinical models. Typically, 2D cell line (CL)-based models are used to screen compounds followed by validation in animal models to generate the evidence needed to design clinical trials. This process incurs a high cost to the research pipeline and still results in high drug attrition rates. This may in part reflect the poor translation of preclinical to clinical results and points to deficiencies in modeling. Previous work from our laboratory shows that the sensitivity of our EOC CLs to carboplatin therapy varies between 2D and 3D *in vitro* models, however it is unclear how these differences align with the *in vivo* response. We hypothesize that 3D models will more closely reflect therapeutic *in vivo* response. The objective of this study was to characterize the carboplatin sensitivity of EOC CLs in 2D and 3D-spheroids and compare them to *in vivo* response using mouse xenografts. We injected mice with 6 different EOC CLs that were treated with 3 different carboplatin concentrations. Tumor volume measurements and immunofluorescence viability stains were used to categorize CLs by their sensitivity. The same CLs were seeded in low attachment plates to form, and thereafter treat, spheroids. Flow cytometry analysis was used to classify CLs by their 50% inhibitory response (IC_{50}). The 2D response (IC_{50}) for these CLs has previously been published. Our results show that therapeutic response changes significantly for a single CL between different systems, and the 3D model was most concordant with the *in vivo* model. Our ultra-resistant CL in 2D became more sensitive in 3D/mouse models. In contrast, the highly 2D sensitive CL became more resistant in our xenograft/spheroid models. The results are important to consider when investing time/funds in drug screening and therapeutic response prediction studies.

Keywords: preclinical models, ovarian cancer, mouse xenografts, spheroids, carboplatin

Table of Contents

List of Tables

List of Figures

List of Supplemental Figures

List of acronyms and abbreviations

2D: two-dimensional

3D: three-dimensional

AKR1C1: Aldo-Keto Reductase Family 1, Member C1

ABC: ATP-binding cassette

BRCA: BReast Cancer

CC3: cleaved caspase-3

ECAD: e-cadherin

ECM: extracellular matrix

EMT: epithelial-to-mesenchymal transition

EOC: epithelial ovarian cancer

FFPE: formalin-fixed and paraffin-embedded

GEM: genetically engineered mouse

H&E: hematoxylin & Eosin

HGS: high-grade serous

HR: homologous recombination

HRD: homologous recombination DNA repair deficiency

HTS: high-throughput screening

IC_{50}: 50% inhibitory response

IF: immunofluorescence

IHC: immunohistochemistry

IP: intraperitoneal

LSM: light sheet microscopy

MDR: multidrug resistance

MMR: mismatch repair

NCAD: n-cadherin

NHEJ: non-homologous end-joining

OS: overall survival

PAN-CK: pan-cytokeratin

PDO: patient-derived organoids

PDX: patient-derived xenograft

PFS: progression-free survival

RCT: randomized controlled trial

SLUG: zinc finger transcription factor SNAI2

SNAIL: zinc finger transcription factor SNAI1

TFI: treatment-free interval

TME: tumor microenvironment

TWIST1: twist-related protein 1

TWIST2: twist-related protein 2

ULA: ultra-low attachment

VEGF: vascular endothelial growth factor

VIM: vimentin

ZEB1: zinc finger E-box-binding homeobox 1

ZEB2: zinc finger E-box-binding homeobox 2

To my husband, Thomas, and my daughter, Mila, who supported me during my studies and who witness my triumphs and challenges

Acknowledgements

I would like to first extend thanks to my research supervisor, Anne-Marie Mes-Masson, and the research associate, Euridice Carmona, who have guided me in the project's inception and evaluation/analysis of results. I am eternally grateful to their support in my career development. I would like to also thank all the research assistants and technicians (Kim Leclerc Désaulniers, Jennifer Kendall-Dupont, Manon De Ladurantaye, Adriana Orimoto) that have trained me and helped with various technical aspects of this project. I would also like to thank the students (Kayla Simeone, Alex Sauriol) in Dr. Mes-Masson's laboratory that have shown kindness and patience in imparting their knowledge and assisting me during my Master's project. I would like to acknowledge the technicians in charge of the research centre platforms I used, namely Molecular Pathology (Liliane Meunier and Véronique Barrès), Cellular Imaging (Aurélie Cléret-Buhot and Isabelle Clément), and Flow Cytometry (Paméla Thibeault). Finally, I would like to thank the funding agencies (Canadian Institute for Health Research, Fonds de recherche Québec-Santé, Centre de recherche du Centre hospitalier de l'Université de Montréal, Institut du cancer de Montréal, Université de Montréal) that have supported this project.

Foreword

As a gynecologic oncology and clinical-investigator trainee, I have witnessed the devastating effects of an ovarian cancer diagnosis. Despite extensive research in the field, few novel therapies have significantly improved the survival of this disease, and a cure is still not in sight. Improving preclinical models are crucial for drug development and an excellent example of translating bench-to-bedside science, hence my choice to dedicate my studies to this project.

Chapter 1 – Introduction and Review of the Literature

Epithelial Ovarian Cancer

Disease Demographics

Epithelial ovarian adenocarcinoma (EOC) is the most lethal gynecological cancer. In 2020, 3100 new cases are projected in Canada and 1950 of these women will die from their disease[1]. Last year, 22,530 women were diagnosed with EOC in the United States and 13,980 died of the disease[2]. Although cure rates are high in early-stage disease (5-year survival of 92.6%), most women are diagnosed at late stages III-IV, and only 30.2% will survive 5 years after diagnosis[3]. This is in part due to the silent nature of this disease, hence its colloquial name 'the silent killer'. EOC is unique in that metastases more commonly occur through direct exfoliation of single or clusters of cancer cells that implant into the peritoneum of the abdominal cavity rather than hematogenous spread with stromal invasion[4]. In this process, many patients develop ascites, a phenomenon defined by the excessive accumulation of peritoneal fluid in the abdomen, that have downstream effects on vital organs related to abdominal compression. For these reasons, many patients die from bowel obstruction due to extensive tumor implants on the peritoneum lining of the bowel and the accumulation of recurrent ascites.

It has now been clear for many years with the advent of molecular genomics that EOC encompasses multiple histotypes namely high-grade serous (HGS), endometrioid, low-grade serous, clear cell and mucinous adenocarcinomas[5]. These 5 subtypes have been categorized in two broad entities; Type I and Type II disease[6]. The former involves the more indolent but chemoresistant subtypes (low-grade serous, mucinous, endometrioid, clear cell) while Type II disease (mostly HGS) tends to be more advanced and aggressive, but chemosensitive at initial

presentation. By far, HGS EOC is the most common histotype[6]. Over 90% of HGS cancers harbor somatic *TP53* mutations and exhibit extensive chromosomal abnormalities[7-9]. Furthermore, compromised homologous recombination due to *BRCA* dysfunction, through inherited germline mutation (see below), somatic mutation or epigenetic silencing[9 10], occurs in approximately 40% of the HGS EOC cases. The prevalence of *TP53* mutations and BRCA deficiency leads to incompetent DNA repair and likely contributes to chromosomal instability, resulting in severely aberrant karyotypes. In general, HGS EOCs are highly heterogenous having widespread inter- and intra-tumoral mutation profiles[9 11]. Its high genomic instability is thought to contribute to the development of innately resistant subclones which may explain why 20% of patients are poorly responsive to first-line therapy[12]. Endometrioid subtypes more commonly involve *PIK3CA* mutations, clear cell carcinoma has *ARID1A* and *PIK3CA* mutations, and low-grade serous types often harbour *BRAF* or *RAS* mutations. Mucinous EOC is a rare subtype that usually contains *PIK3CA* and *KRAS* mutations[6].

Hereditary syndromes associated to EOC

Fifteen percent of all EOCs are associated with a hereditary predisposition. The BReast CAncer (*BRCA*) and mismatch repair (*MMR*) autosomal dominant genes make up the bulk of these predispositions. The former was first discovered in its association to breast cancer risk[6]. Mutations in the *BRCA* 1 and 2 genes are mostly found in the HGS subtype, where 15-20% of patients carry a germline mutation. Tumors that share molecular features of *BRCA* mutant tumors, but are not *BRCA* mutated, are thought to carry a BRCAness phenotype with potential similar therapeutic susceptibilities[13]. Other less common mutations exist, *BRIP1*, *RAD51C*, *RAD51D*, that carry this BRCAness phenotype and have been associated with an increased risk of EOC and an impact on patient management[14]. For this reason, currently, there is consensus

that all patients with this subtype should undergo germline genetic testing[6]. There is current research exploring the option of tumor testing first, and then genetic testing/counseling for positive cases, however this is investigative at the moment[15]. Because of its hereditary nature and the access to preventive treatments, a confirmed germline mutation would trigger genetic testing to first-degree relatives. This is important as, without a therapeutic cure, prevention is the only way to potentially 'cure' these patients. The lifetime risk of developing ovarian cancer is 44% in BRCA1 and 17% in BRCA2 mutation carriers[6]. The current National Comprehensive Cancer Network (NCCN) guidelines recommend that these patients undergo prophylactic risk-reducing surgery by 35-40 years with the possibility to delay bilateral salpingo-oophorectomy for BRCA2 mutation carriers to 40-45 years, given the later diagnosis in this group of patients[14]. Furthermore, the BRCA status is important for therapeutic option based on the notion of synthetic lethality discussed below.

The other important hereditary predisposition associated with EOC risk is Lynch syndrome[6]. It involves absent MMR proteins due to MMR gene mutation that results in microsatellite instability. As in endometrial and colon cancer, the 4 main proteins associated are PMS2, MLH1, MSH6 and MSH2[16]. Typically, Lynch syndrome is more commonly associated with endometrioid or clear cell EOC subtypes[17 18]. As such, therapeutic options specific to patients with MMR protein deficiencies are available and will be discussed below.

First-line Treatments and Current Challenges

Traditionally, the standard treatment of advanced EOC involves a combination of cytoreductive surgery with platinum-based chemotherapy[6]. Unfortunately, despite extensive research in the field, very few new treatments have significantly changed the overall prognosis for these patients.

The current standard of care for Type II disease and advanced Type I disease is intravenous carboplatin (a DNA cross-linking compound) and paclitaxel (a microtubule stabilizing drug) systemic therapy (with or without bevacizumab, an anti-angiogenic agent targeting vascular endothelial growth factor A, VEGF-A) which can be administered through various routes[6]. Traditionally, this treatment combination is offered as adjuvant therapy but, numerous randomized controlled trials (RCTs) in the last ten years have demonstrated the non-inferiority of its use in the neoadjuvant setting followed by interval debulking surgery which can be defined as surgery performed between cycles of chemotherapy[19-21]. The majority of patients in these trials are of the HGS subtype. Furthermore, in certain cases, patients with optimal/complete cytoreduction are eligible for intraperitoneal (IP) therapy through an IP port[22], although the previously reported survival advantage has been put into question[6]. Hyperthermic IP cisplatin therapy can now be given at the time of interval debulking surgery if there is evidence of initial response to neoadjuvant platinum-therapy[23]. However, these modified regimens have at most improved overall survival (OS) by one year but have not changed the cure rates for these patients.

In regard to targeted therapy, bevacizumab, in the first-line setting (with maintenance), has demonstrated a progression-free survival (PFS) benefit[24]. An OS benefit was seen in patients with poorer prognostic features[25]. Furthermore, in rarer subtypes of ovarian cancer that are often chemoresistant, other targeted therapies are being considered. In low-grade serous ovarian cancer, anti-hormone therapy will be evaluated in an upcoming trial GY019 (NCT04095364) as adjuvant therapy in lieu of standard carboplatin/paclitaxel after cytoreductive surgery. In MMR deficient ovarian adenocarcinomas, immune checkpoint inhibitor pembrolizumab, a PD-1 receptor inhibitor, is approved for advanced disease[17]. In the Phase II trial Keynote-158, 6% of patients had ovarian cancer and these patients experienced a 33% overall response rate[26].

Maintenance Therapy

Maintenance therapy is any treatment received after completion of first-line treatment with the goal of delaying or preventing recurrence. There is no data to support the use of bevacizumab as maintenance if not used in the primary treatment regimen. After first-line therapy, maintenance treatment should be given to patients as well. In 2018 and 2019, the poly (ADP-ribose) polymerase (PARP) inhibitors (PARPis), olaparib and niraparib, were shown to demonstrate a significant PFS benefit as maintenance therapy after first-line treatment[27 28]. PARPis target the protein PARP 1/2 involved in repairing damaged DNA. Olaparib was studied in BRCA mutated tumors only[28], whereas niraparib was evaluated in sporadic EOC as well[27]. This led to FDA approval of these drugs and is now part of standard treatment. In low-grade serous stage II-IV disease, maintenance anti-hormone therapy such as letrozole improves PFS[29].

Second-line Treatments and Challenges

As previously mentioned, although many patients initially respond to treatment, most patients will inevitably experience relapse and will develop lethal metastatic chemoresistance (acquired resistance). Patients are categorized according to their therapy-free interval (TFI), and with platinum-based chemotherapy, they are labelled as platinum-sensitive, -resistant or -refractory for those that have a TFI of > 6months, 1-6 months and < 1month, respectively[30]. It is currently the only good predictive marker of response to second-line therapy[31]. However, response is inevitably not sustained, and curative treatment becomes impossible in 3/4 of relapsed cases, hence the collective effort in the research field to better understand this disease to find more effective treatments[6].

Unfortunately, most women will die from their disease after cancer relapse. Options currently available to these patients include secondary cytoreductive surgery, chemotherapy, targeted therapy, immunotherapy, anti-hormone therapy, and most importantly clinical trials. Secondary debulking surgery followed by chemotherapy can be offered to a select group of patients who fit the Arbeitsgemeinschaft Gynaekologische Onkologie (AGO) criteria: minimal (< 500mL) ascites, complete initial resection, relapse at least 6 months from platinum-treatment and good performance status[32]. However, most patients do not fulfill these criteria and therefore need systemic treatment. Traditionally, for platinum-free interval > 6 months, second-line chemotherapy combination of carboplatin with either liposomal doxorubicin, gemcitabine, and paclitaxel are the preferred regimens. In the setting of platinum-resistant or -refractory disease, these latter treatments are given as single agent chemotherapy.

Based on phase II trials[33], bevacizumab as single agent is an option for platinum-sensitive or -resistant disease (especially those with ascites). Combination with some of the previously mentioned regimens for platinum-sensitive[34 35] or -resistant[36] disease can be given as well. PARPis (with or without bevacizumab) are being evaluated in RCTs for their use as second-line agents[37]. Maintenance therapy with PARPi, however, can be given to BRCA mutated[38 39] or BRCA wildtype[39] platinum-sensitive HGS/endometrioid tumors after response to second-line treatment. As previously mentioned, targeted therapies such as Pembrolizumab can be given to advanced or metastatic MMR deficient tumors[17 18].

EOC Biomarkers

To guide the choice of anti-cancer therapies, a large number of biomarkers have been studied as indicators of an increased probability of drug responses in EOC patients[40]. These include

apoptosis-related proteins, transcription factors, epithelial-to-mesenchymal transition (EMT) proteins, growth factor receptors, immune-related markers, among others. However, the majority of them are not clinically useful as they have low sensitivity/specificity[41]. Furthermore, there are no current standard guidelines for the reporting of these biomarkers which makes reproducibility difficult. For this reason, national and international consortia have been developed to pool reviewed clinical and biomarker data on EOC patients[41]. One of the most well-studied blood biomarkers is the CA125 mucin glycoprotein, however, its use is limited as it is not validated for screening[42] or surveillance[43]; rather its use lies in determining response to treatment and identifying recurrence[43 44]. Studies combining CA125 levels with other candidate proteins may offer better sensitivity and specificity, but have not reached clinical significance[45]. Finally, there is also much promise with liquid biopsies that require small amounts of starting material such as circulating tumor cells, circulating tumor DNA and micro RNA[41]. These may have potential use in the setting of prevention, early detection, response to treatment and surveillance.

Furthermore, somatic and germline DNA damage repair biomarkers are currently used to correlate with response to platinum chemotherapy and drugs targeting the DNA repair pathway. An excellent example of this is the discovery that HGS patients with somatic/germline BRCA mutations have an increased PFS and OS with PARPi, such as olaparib, as maintenance therapy after first-line therapy (SOLO-2 trial)[38 46]. Somatic tumor testing is a quick tool that detects 5-10% of BRCA cases potentially eligible for PARPi treatment and would have not otherwise been identified[47 48]. Conversely, germline testing can detect 5% of cases missed on tumor testing[28]. A combination testing is now recommended in order to ensure that all patients are identified[15]. More recently, biomarker panels have broadened to include more mutations and a homologous recombination DNA repair deficiency (HRD) scoring system was created by several companies

such as Myriad Genetics and Foundation Medicine[49] and have been used in RCTs. Another PARPi, niraparib, was thus further evaluated not only in the setting of BRCA mutation, but also in BRCA wildtype patients with positive HRD scores, and BRCA wildtype HRD-negative scores[27 39].

Another example of biomarkers used in EOC is the estrogen- or progesterone-receptor (ER/PR) status in low-grade serous disease as it carries a high positive incidence, which had led to the use of anti-hormone therapy, such as letrozole, in this EOC subtype[29 50]. There is a better OS associated with higher ER score[50], hence the rationale for the previously mentioned GY019 trial design[51]. Moreover, microsatellite instability is a biomarker that has been explored in MMR deficient tumors including ovarian cancer[26]. PD-1/PD-L1 status are other biomarkers explored to predict the response of immunotherapy in clear cell EOC[52-54]. Finally, there is also much promise with liquid biopsies that require small amounts of starting material such as circulating tumor cells, circulating tumor DNA and micro RNA[41]. These may have potential use in the setting of prevention, early detection, response to treatment and surveillance.

Although the theranostics approach has led some of the aforementioned discoveries, they have their limitations. In the case of HGS EOC, half of BRCA mutated patients do not derive a clinical benefit within the first months of treatment to olaparib and 1/3 of wild-type BRCA tumors respond to olaparib[55 56]. With the high cost of these targeted therapies, this poses a challenge in precisely identifying those that would benefit from these treatments and those who will not respond. In order to address this, reliable and practical preclinical models are needed to study drug response and putative biomarkers.

Preclinical Models for Drug Screening and Prediction

A significant amount of money has been invested in discovering new cancer treatments with limited focus on the actual experimental models used to test these agents[57]. The current drug discovery pipeline is dependent on preclinical models which mostly consist of 2D systems, because of time and cost efficiency. As one of the traditional models used in oncology research, patient-derived immortalized cell lines are grown in 2D plastic dishes. They are derived by multiple passaging to enzymatically filter out stromal cells in order to isolate epithelial cells. It is furthermore devoid of an extracellular matrix and loses most of the cell-to-cell interactions seen in the original tumor tissue. Primary cultures have also been used but have a finite use and have their own culture challenges[58].

2D preclinical models have allowed researchers to understand the molecular biology of EOC and make important discoveries in regard to cancer-specific targets and new therapies. However, while this form still remains today the primary method of preclinical testing, attrition rates of anti-cancer drugs continue to be high and EOC survival remains low. This is in part due to poor translation of preclinical testing into clinical trials. In fact, only 10% of drugs actually make it to Phase I clinical trials and 15% of these qualify for Phase III[59]. More recently, the use of 2D models for preclinical oncology research has received increasing criticisms. In particular, it has been noted that this method of culturing puts into question the proper representation of the tumor heterogeneity due to selective pressures on cells, that it lacks an immune component and that it lacks interaction with the tumor microenvironment (TME) be it the extracellular matrix (ECM), tumor cell-stromal cell interactions, or additional important components[60]. Furthermore, many of these cell lines were characterized primarily in their 2D form, and thus little is known about differences in phenotype, protein expression, cell viability and other important biological markers

when cultured in other model systems. A summary of the advantages and disadvantages of different cancer experimental models can be found in Table 1.

Table 1. **Advantages and Disadvantages of Different Model Systems in EOC**

	2D	**3D**	***In vivo***
Advantages	- Convenient - Economical - Homogenous cells - Large panel of cell lines - Control of culture conditions	- Increased tissue complexity - Inclusion of TME elements - More accurate chemical gradients (O2, nutrients, drug) - Co-culture possible	- Increased tissue complexity - Stroma and vascular interactions - Pharmacokinetics studies - Patient-derived xenografts (PDX) show tumor heterogeneity in early passage
Disadvantages	- Lack 3D architecture - Lack ECM - Selection of subclones - Non-physiological conditions (culture, mechanical surface) - Short-term use (primary cultures)	- 3D adapted measurements limited (metabolic state of cells measurement using reagents and phenotypic response using microscopy[57]) - Requires optimization - Dependent on sample availability if fresh tissue-based model (ex-vivo models) - Avascular[61]	- Cost - Enhanced animal expertise - Low throughput screen - Mice are typically immunodeficient - Latency time for tumor growth - Xenograft engraftment failure[12] - Murine stroma - Orthotopic tumors require imaging analysis - Subcutaneous tumors don’t allow study of metastases - PDXs rely on fresh tissue availability - Endogenous mouse hormones (estrogen)[62] - Clinical translation of xenografts still under study

Alternatively, animal models have also been vital to preclinical EOC research[63 64]. Typically, they are used to validate *in vitro* discoveries and to assess physiological response and pharmacokinetics. By far the most common type of *in vivo* cancer model used is mouse xenograft (heterotopic or orthotopic) models. In the case of EOC, they are usually performed through subcutaneous or intraabdominal injection of immortalized cancer cell lines into immunodeficient mice. Therapeutic responses are often ascertained through a combination of tumor size/weight, mouse survival and histopathology. This preclinical model is expensive and can incur high costs with unnecessary animal experimentation if used as a screening model. As this animal model also has its shortcomings (discussed in Table 1), newer *in vivo* models have been developed such as patient-derived xenografts (PDX) and genetically engineered mice (GEMs) (as reviewed in[65 66]). However, there is still long ways to go with some of these newer models as they remain investigational, costly and laborious.

An ideal preclinical model has optimal physiologic relevance for a drug screening/prediction platform, with high-throughput screening (HTS), downstream analysis compatibility, translatable in a clinically relevant timeframe, and affordable[67]. It is important to understand that currently there does not exist a single preclinical model that can precisely answer all possible questions in the field of oncology (pathogenesis, target validation, drug selection, resistance mechanisms, etc.)[66]. When deciding on which preclinical model to use it is important to consider the scientific question and the endpoints of a study.

To bridge the gap between the shortcomings of 2D model and animal experimentation, there has been a shift to further develop 3D models. In the case of EOC, multicellular tumor spheroid 3D *in vitro* models have been extensively developed as they reflect a physiological event in the natural history of this disease. As previously discussed, clusters of cells (i.e. spheroids) of

approximately 50-750µm detach from the original tumor and either float freely or implant themselves on the peritoneal surface[68]. These clusters of cells are resistant to anoikis through changes in matrix stiffness and EMT that increase survival more than single cell detachments[4 69]. Cancer stem cells have also been found in ascites fluid and, through their chemoresistance and ability for self-renewal, they are believed to contribute to recurrence of the disease[67].

In vitro spheroids can be generated using fresh samples or cell lines. Multiple studies in EOC and other cancers have shown that 3D culture is physiologically different from 2D cultures. Desmosomes and dermal junctions, secretion and deposition of ECM proteins and proteoglycans create the cellular interactions within spheroids to enhance its compactness[70]. Spheroids model avascular or poorly vascularized tumors and regions with poor oxygenation and nutrients[71]. These changes will usually be observed when the spheroid is higher than 200-500µm depending on culture conditions[72 73]. Overall, this model mimics the structural (cell-cell interactions), the biological (gene expression profile, tumor cell heterogeneity), the chemical (nutrient and oxygen gradients) features of an *in vivo* system and allows the possibility of co-culturing with cancer-associated cells to more closely resemble the TME[57 74-76]. The scientific literature is rich on methods of spheroid formation, each with their advantages and disadvantages (see Table 2). Other elements can be added to the spheroid model such as scaffolds, ECMs and hydrogels which have shown to influence spheroid size and drug penetration[61 77 78].

Table 2. **Methods of Spheroid Formation**

Methods	**Options**	**Advantages**	**Disadvantages**
Non adherent plate (static)	Option of adding ECM scaffold[79] (anchorage)[1,2] Natural[3] (Collagen) or Synthetic (PLA, PGA)	- Rapid spheroid formation - Uniform spheroids - Easy handling - Long-term culture - Inexpensive - High-throughput screening	- Difficult long-term culture[73] - High plate cost
Hanging droplet (static)		- Uniform spheroids	- Short-term culture - Limited harvesting - Limited sample throughput[71 73]
Spinner flasks/rotary vessel (agitation based)		- Long-term culture - Mass production - Easy handling	- Non-uniform spheroids - Exposure to sheer forces - High cost - Time-consuming[70]
Microfluidics		- Rapid spheroid formation - Requires less starting material (tumor cells) - Formation, testing and analysis on same chip - Well-defined gradients	- Collection more difficult[73]

[1]May incur difficulties in effective collection and separation of spheroid from scaffold
[2]Allows ECM-cell interactions in the spheroid
[3]Batch to batch composition differences

Therapeutic Response across Model Systems

An important part of experimental model development is the methodology used for analysis. One of the advantages of 2D preclinical models is that there exist multiple analytical methods for various endpoints for drug screening and therapeutic response prediction. These include cell proliferation and metabolic assays, clonogenic assays, flow cytometry, immunohistochemistry and immunofluorescence. Much effort has been focused on developing 3D models for HTS to improve cost- and time-efficiency. Current methods to analyze drug screening and response mostly rely on dissociating the 3D model to use 2D model analysis methods, histopathology, measures of metabolic activity and spheroid size[80-82]. The latter however does not always reflect the viability status of the cells in the spheroid and may be a less accurate representation of chemoresponse, as we have previously shown[83].

With different model systems being developed, the study of different cellular parameters such as phenotype, protein expression and viability have been carried out. A number of these cellular processes have been found to be different simply by culturing the same tumor cells in 3D compared to 2D. These changes occur at the level of EMT genes, epigenetic changes, DNA integrity and cellular stress pathways[84]. *Lawrenson et al* observed changes in these features in normal ovarian surface epithelial primary tissue between its 2D and 3D model. The latter more closely resembled the primary tissue characteristics[85]. Encouragingly, there is evidence from gene expression analyses in EOC cell lines that results are more similar between 3D spheroids and ovarian xenograft tissue, than in monolayers[86]. Moreover, analysis of the cells within a 3D spheroid have identified three principal layers within this model: proliferative outer layer, a quiescent middle layer and a hypoxic/necrotic inner layer[74 76 87]. *In vivo* tumors share some of these features as well.

As 3D models were being studied, many researchers became interested in understanding how a model system can affect therapeutic response with different cytotoxic agents. In the last decade, most publications have concluded that cells in a 3D model are more resistant to treatment than in its 2D model[74 75 88-95]. This may explain the poor translation of preclinical results into clinical trials with different drug efficacy and dosing[96]. *Flick et al* validated the ability of *in vitro* chemosensitivities of ascitic fluid spheroids to predict patient responses in a series of 13 ovarian cancer cases[97]. In the case of 3D multicellular spheroid, proposed reasons for discrepancies include diffusion of oxygen/nutrients/drugs, physical barriers from cellular links, hypoxic/necrotic cores, changes in gene expression, cell behavior changes, etc[74 76 79 80 88 98]. Compared to monolayer cultures, spheroids and tumors have initial exponential growth that declines over time with an increase in nonproliferating and necrotic cells[76]. Previous studies have shown a higher proportion of cells in G0-G1 and a lower portion of cells in S and G2-M phases supporting the cell layers of this model[79]. Drug effectiveness relies on cells' replicative activity and drug distribution[70]. This may explain why cytotoxic agents that target replicating cells may be dysfunctional in the inner two layers of a spheroid especially with increasing diameters[79 80]. Furthermore, avascular or poorly vascularized inner tumor cells are exposed to lower levels of drug concentration as it mostly accumulates in the outer proliferating layer[90]. This effect is accentuated with increasing spheroid cell density/diameter and the gap in drug accumulation between inner and outer cells widens[90]. Furthermore, low oxygen areas of the spheroid reduce production of reactive oxygen species which affects the efficacy of anti-cancer drugs[70]. Changes in gene expression can also affect response to therapy. *Paullin et al* reported an upregulation of the gene *AKR1C1* (Aldo-Keto Reductase Family 1, Member C1), involved in detoxification, in EOC cells that is known to be associated with platinum-resistance[84]. 2D models are not exposed to these same barriers that change the diffusion pattern and action of drugs.

Rationale, Hypothesis and Objectives of this Study

Our group has recently reported results of a study comparing carboplatin chemosensitivity between *in vitro* models[83]. Using four of our laboratory's EOC cell lines, a 2D model was compared to two different 3D models. Results showed that response to chemotherapy varied significantly from one model to another for the same cell line and furthermore that this change did not follow the same trend across cell lines. This puts into question the reliability of EOC preclinical models with such variability seen between *in vitro* models.

More importantly, it is currently unclear whether one of these *in vitro* models accurately reflects the *in vivo* response. Our hypothesis is that a 3D microenvironment would more closely approximate the *in vivo* therapeutic response. Given that EOC clinical prognosis is based on platinum sensitivity[30], carboplatin treatment in three different model systems were compared to one another. The primary objective of this study is to characterize the sensitivity of our EOC cell lines to carboplatin in 2D monolayers and 3D multicellular spheroids and compare them to their *in vivo* response using our mouse xenograft model (Figure 1). Our results highlight the variability in therapeutic response across model systems and the importance of testing therapies using multiple preclinical models prior to clinical trial design.

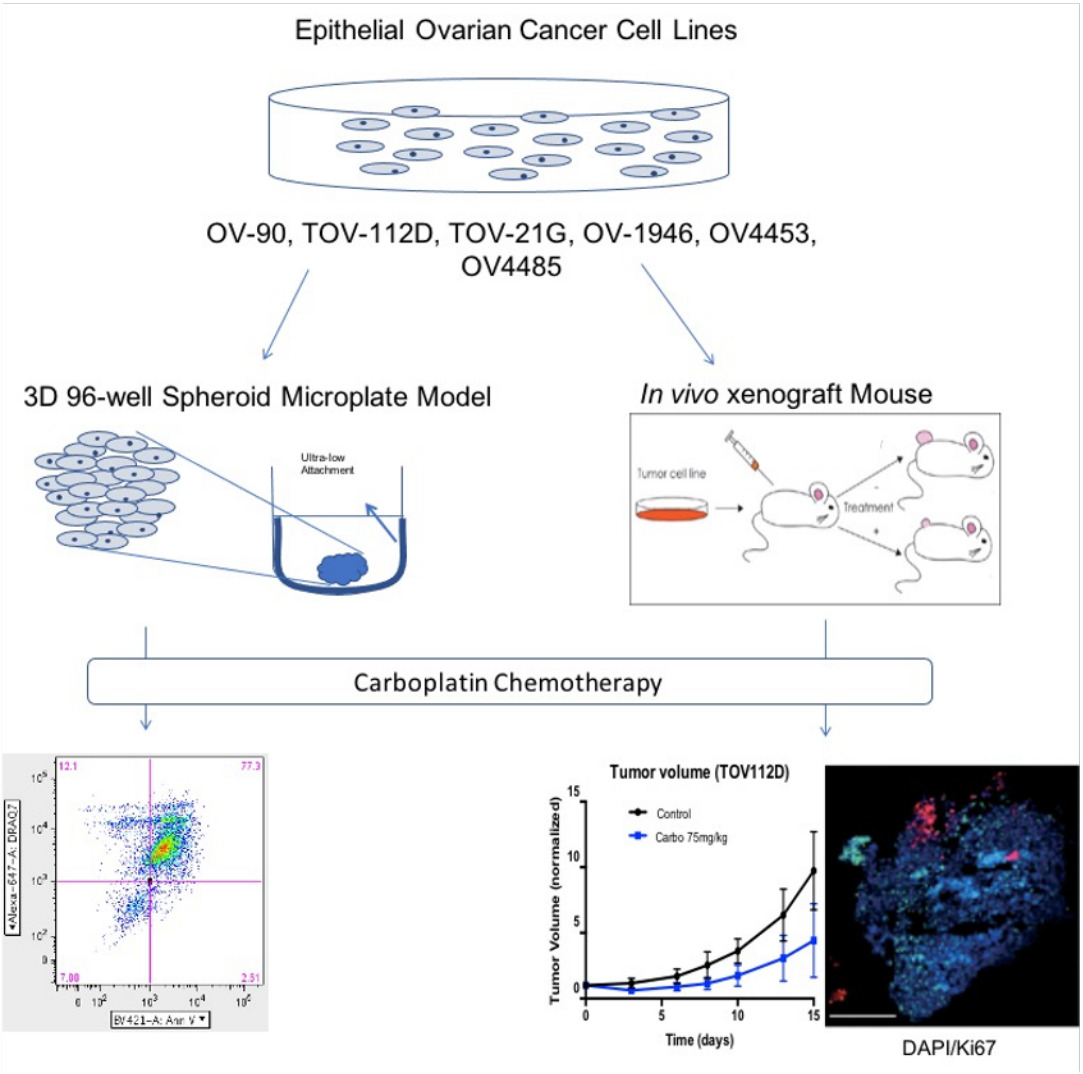

Figure 1. **Schematic illustration of study design**

Chapter 2 – Methodology

Cell lines

Six of our laboratory's patient-derived EOC cell lines of varying carboplatin (2D) sensitivity and able to form tumor xenografts were used in this study: OV-90, OV4485, OV4453, TOV-21G, TOV-112D and OV-1946[99-102]. Mycoplasma testing and STR analysis were performed for all cell lines. These cell lines originate from either patient tumors (TOV) or ascites (OV). OV4485 and OV4453 are BRCA1 and BRCA2 mutated cell lines, respectively. Cells were cultured in completed OSE medium (Wisent, QC, Canada) supplemented with 10% fetal bovine serum (Wisent), 2.5 ug/mL of amphotericin B (Wisent) and 50ug/mL of gentamicin (Wisent). Cells were cultured in their ideal growth parameters. OV-90, TOV-21G, TOV-112D and OV-1946 cells were maintained in 100mm dish with 21% O_2, 5% CO_2 at 37°C, and OV4485 and OV4453 were kept at 7% O_2, 5% CO_2 at 37°C. All cells were passaged when they attained 90% confluence and all experiments were carried out with cells between passage 70 to 80.

Xenograft model

Establishment of tumor model

NOD.Cg-Rag1tm1Mom Il2rtm1Wjl/SzJ immunodeficient female mice (The Jackson Laboratory, JAX stock #007799)[103 104] were used to form tumors with our 6 cell lines. A total volume of 200µL consisting of a suspension of 1 x 10^6 cells in 100µL cold Dulbecco's phosphate-buffered saline (D-PBS) (Wisent) and 100µL of Matrigel® Matrix (Corning Inc., NY, USA) was injected subcutaneously in the flank of each mouse for the TOV-112D, TOV-21G and OV-90 cell lines,

while 5 x 10^6 cells were injected for OV-1946, OV4453 and OV4485. Eight mice were used for each of the four following carboplatin treatment groups per cell line: 0 mg/kg, 25 mg/kg, 50 mg/kg and 75 mg/kg (see below for treatment dose optimization). Carboplatin treatment was initiated once tumors attained an average of 200mm^3 (drug effects can vary if below 200mm^3)[66]. Mice were between the ages of 11-24 weeks at the start of treatment. All animal procedures were performed in accordance with the guidelines for the Care and Use of Laboratory Animals of the CRCHUM and approved by the Animal Ethics Committee, i.e., the *Comité institutionnel de protection des animaux (CIPA)*. Mice were given dietary supplementation (DietGel® Recovery 72-06-5022 and DietGel® Boost) twice weekly and tumors were measured in three dimensions (length, width, depth) with calipers 2-3 times weekly by the same animal technician. Furthermore, to alleviate the known negative side effects of carboplatin treatment, anti-nausea medications (see optimization protocol below) were given one hour before the chemotherapy dose as well as 24 and 48 hours following carboplatin treatment. Mice were sacrificed at the end of the treatment period or if ethical limits were attained. At the end of the experiment, tumors were collected, measured and were formalin-fixed and paraffin-embedded (FFPE). For each mouse, FFPE tumor blocks were cut into 4µm sections for histological Hematoxylin & Eosin (H&E) staining to distinguish cell nuclei and ECM/cytoplasm, respectively. This provided information on the general tissue architecture and the identification of epithelial and stromal structures.

Optimization studies for drug administration

A first pilot study was performed with weekly IP carboplatin cycles of 100mg/kg up to three cycles so as to not exceed the known LD50 of 118mg/kg[105]. A second pilot study was performed with a lower dose of 75mg/kg, given the high mortality rate with 100mg/kg, and two anti-nausea

medications (1mg/kg of maropitant and 0.8mg/kg of ondansetron) were given subcutaneously 3 times weekly to aid with malnutrition secondary to nausea observed in the first pilot study.

3D spheroid formation

Spheroid formation was completed using 96 concave-bottom ultra-low attachment (ULA) microplates (Corning 4515/4520). This technique allows for uniformly homogenous formation of spheroids in a short time frame[61 74]. Previous work has shown that with this method EOC cell lines form more compact spheroids in a shorter period of time than with traditional hanging droplet method[71 99 83]. For all six cell lines, 2000-2500 cells in 100µL of complete OSE medium were seeded in each well to attain approximately 500µm diameter spheroids at 48 hours of formation. At this time, carboplatin treatment was administered for 24 hours with a 24-hour recovery period. Therefore, the experiment lasted a total of 96 hours post-seeding. For each condition and cell line, 20 spheroids were used, to provide two replicates of 10 spheroids. Plates were centrifuged at 1000rpm for 5 minutes at room temperature. Spheroids were allowed to form over 48 hours for optimal cell aggregation/adhesion time in their respective ideal incubation conditions (see section Cell Lines). Spheroids cultured for shorter periods do not have sufficient time to develop model-specific cell-cell and cell-ECM interactions[71 73].

Carboplatin Treatment

Based on previously performed pilot studies, carboplatin (Hospira Healthcare Corporation) treatment in our xenograft model was given once weekly IP at doses of 25, 50, and 75 mg/kg for

up to a total of 6 cycles. The carboplatin vehicle, 0.9% NaCl solution, was used for the control group.

Optimization studies were performed with spheroids to determine a carboplatin treatment range. Thereafter, spheroids in the ULA plates (cultured in 100µL) were treated with an additional 100µL of three different in-well concentrations of carboplatin (range, 0 to 3000µM). 100µL of complete OSE medium was used for the control group. Spheroids were treated for 24 hours followed by a 24-hour recovery period. This chemotherapy incubation time was chosen based on the literature suggesting that 24h of drug exposure is required to disintegrate the outer proliferative layer and penetrate the spheroid[90 91 106]. A 24-hour recovery was chosen to mimic the physiologic metabolism of the drug and previous studies demonstrating the effect of chemotherapy after its removal[91 107].

Flow cytometry analysis

After the carboplatin treatment and recovery period, 10 spheroids (one replicate) were pooled per condition and dissociated with trypsin-EDTA (0.05%) for 30-45 seconds to obtain single-cell suspensions. In our pilot studies, we observed that this dissociative agent offered the overall highest cell viability for all cell lines compared to mechanical dissociation or other agents such as collagenase, Accutase and GENTLEMACS. Single cells were then labelled with LIVE-DEAD (LIVE-DEAD™ Fixable Aqua Dead Cell Stain Kit, Thermofisher L34957) stain (1:100 dilution) to detect live and dead cells. After an incubation period between 15-45 minutes at room temperature, the stained cells were analyzed by flow cytometer (LSR-Fortessa, BD Biosciences) within 2 hours of staining, using 405nm excitation, and fluorescence emission was monitored at 525nm. The data collected from each acquisition was analyzed using FlowJo (FlowJo, LLC,

Ashland, USA) by gating the Front/Side Scatter cell population, removing doublets and identifying two main cell populations, dead cells (stained) and live cells (non-stained). Normalized live and dead cell rate could then be plotted from which dose-response inhibition curves, with respective IC_{50}, were generated using GraphPad Prism 6 software.

Immunofluorescence and Immunohistochemistry

FFPE tumor blocs were cut into 4µm sections for immunofluorescence (IF) and immunohistochemistry (IHC) staining to identify cell population composition and viability. Antibodies used for IF included DAPI for nuclei detection and Ki-67 for cell proliferation. Antibodies used for IHC included DAPI for nuclei detection, Ki-67 for cell proliferation and cleaved caspase-3 (CC3) for apoptosis. IF/IHC slides were stained using the BenchMark XT automated stainer (Ventana Medical System Inc., Tucson, AZ). Antigen retrieval using secondary antibodies was carried out automatically with the Cell Conditioning 1 (VMSIl #950-123) for 30 minutes (CC3) or 60 minutes (Ki-67). Rabbit anti-Ki67 (1:200) antibody (RM9106, Thermo Scientific) and rabbit anti-CC3 (1:500) antibody (9661, Cell Signalling Technology, Massachusetts, USA) were dispensed manually. The slides were incubated at 37°C for 60 minutes and developed using the Ultra-View DAB detection kit (VMSI#760-091). All sections were scanned with a 20 x 0.75 NA objective with a resolution of 0.3225µm (bx61vs, Olympus, Toronto, Ontario).

Stained tumors were quantified using VisiomorphDP software (VisioPharm, Denmark). IF filters used for DAPI antibody and anti-Ki-67 were DAPI and TRITC, respectively. The IF quantification of Ki-67 was performed by 1) detecting and calculating the total tissue core surface

area through the DAPI channel, 2) detecting and calculating the total area of Ki-67 positive cells, 3) calculating the ratio of the area in (2), Ki-67, over the area in (1), tissue core. Quantification cut-offs were used to categorize cell lines according to response to carboplatin therapy.

Statistical Analyses

Values are expressed as the means ± standard error of the mean (SEM), derived from at least three independent experiments in the case of 3D-spheroids and, on average, 8 tumors per condition per cell line for the xenograft model. Comparison between multiple groups (different carboplatin concentrations) was determined by one-way ANOVA comparison test. 3D IC_{50} was calculated by transforming all concentrations into logarithms, normalizing the response, and performing nonlinear regression analysis (dose-response inhibition equation – variable slope). P values <0.05 were considered significant. All statistical analyses were done using GraphPad Prism 6 software (GraphPad Software Inc., San Diego, CA).

Chapter 3 – Presentation and Analysis of Results

2D Models

The selection of the 6 EOC cell lines was based on two important factors: the ability to form tumors in immunodeficient mice and their 2D carboplatin chemosensitivity category (Table 3). These cell lines have been extensively characterized in 2D in previously published articles[99-102] and represent the diverse range of EOC subtypes (endometrioid = TOV-112D, clear cell = TOV-21G and HGS= OV-90, OV-1946, OV4453, OV4485). Their 2D platinum-sensitivity obtained by clonogenic assays was used in this study to arbitrarily categorize the cell lines as either sensitive, intermediate or resistant based on their IC_{50}. Cell lines that had an IC_{50} below or equal to 1μM are considered sensitive, those between 1-10μM are intermediate and those above 10μM are resistant.

Table 3. **2D carboplatin sensitivity (clonogenic assay)**

Cell line	**EOC histology subtype**	**Origin of cell line**	**IC_{50} (μM)**	**Chemosensitivity**	**References**
OV4453	High-grade serous	ascites	0.23±0.074	Sensitive	[99]
TOV-21G	Clear cell	tumor	1.0±0.23	Sensitive	[101 102]
OV-1946	High-grade serous	ascites	3.4±0.18	Intermediate	[100]
OV4485	High-grade serous	ascites	6.1±0.27	Intermediate	[99]
TOV-112D	Endometrioid	tumor	13.4±	Resistant	[101 102]
OV-90	High-grade serous	ascites	31.8±5.4	Resistant	[101 102]

3D Spheroid Model

All 6 EOC cell lines formed spheroids in ULA plates (See Figure 2). OV-90 and OV-1946 formed compact spheroids. TOV-112D, TOV-21G, OV4485 and OV4453 formed dense

aggregates. To demonstrate that the cells in the spheroids remain proliferative throughout the experiment period, we performed IHC staining (with CC3 for apoptotic cells and Ki-67 for proliferative cells) for spheroids at 48 hours (time of spheroid formation) and 96 hours (end of experiment) (Figure S1 in Appendix). In general, the cells in spheroids stain strongly for Ki-67 at both time-points with low expression of CC3 demonstrating that they remain proliferative throughout the treatment course.

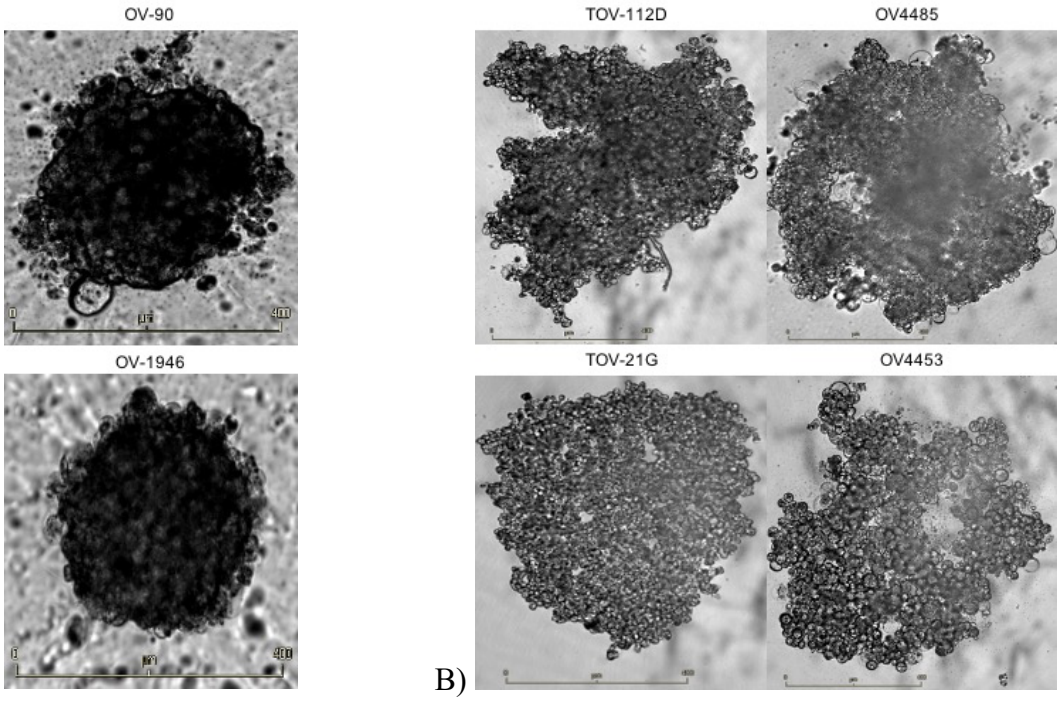

Figure 2. **3D spheroids grown in ULA 96-well spheroid microplates.**

2000 cells seeded and grown for 48hr. **A)** OV-90 & OV-1946 forms round compact spheroids. **B)** TOV-112D, TOV-21G, OV4485 & OV4453 forms dense aggregates. Scale bar = 400µm

Using a LIVE-DEAD aqua stain, flow cytometry was carried out to determine live and dead cell rate after spheroid carboplatin treatment (Figure 3A, Figure S2 in Appendix). IC_{50} were generated using dose-response inhibition analyses (Figure 3B). In all cell lines, the 3D IC_{50} values were significantly higher than that seen in 2D model. However, the fold change in chemosensitivity between the 3D and 2D varied significantly depending on the cell line (Table 4). Cut-off for

resistance to carboplatin treatment was based on response to the physiologic conversion of maximum plasma concentration of carboplatin received by patients, which is 300μM[108]. This estimated calculation is based on a dose of 300mg/m2 of carboplatin, a body surface area of 1.7m2, a total blood volume of 4.7L and the carboplatin molecular weight of 371249 mg/mol. Response to doses below 100μM were considered sensitive. Response in between were considered intermediate. Therefore, OV-1946 was categorized as sensitive, TOV-21G and OV-90 as intermediate, and TOV-112D, OV4453 and OV4485 as resistant.

A)

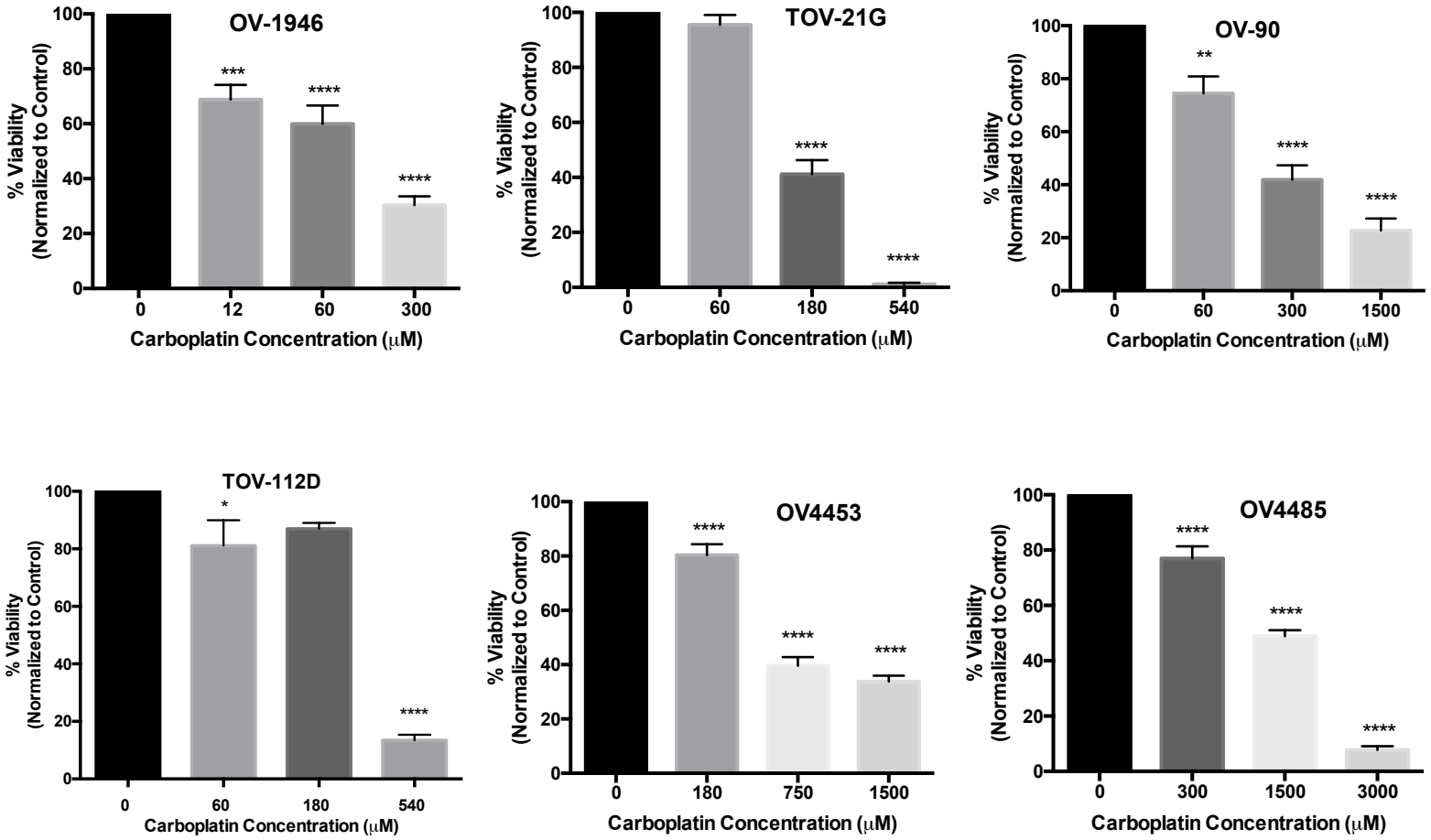
OV-1946
% Viability (Normalized to Control)
Carboplatin Concentration (μM)
0
12
60
300
***
****
****
TOV-21G
0
60
180
540
****
****
OV-90
0
60
300
1500
**
****
****
TOV-112D
0
60
180
540
*
****
OV4453
0
180
750
1500
****
****
****
OV4485
0
300
1500
3000
****
****
****

B)

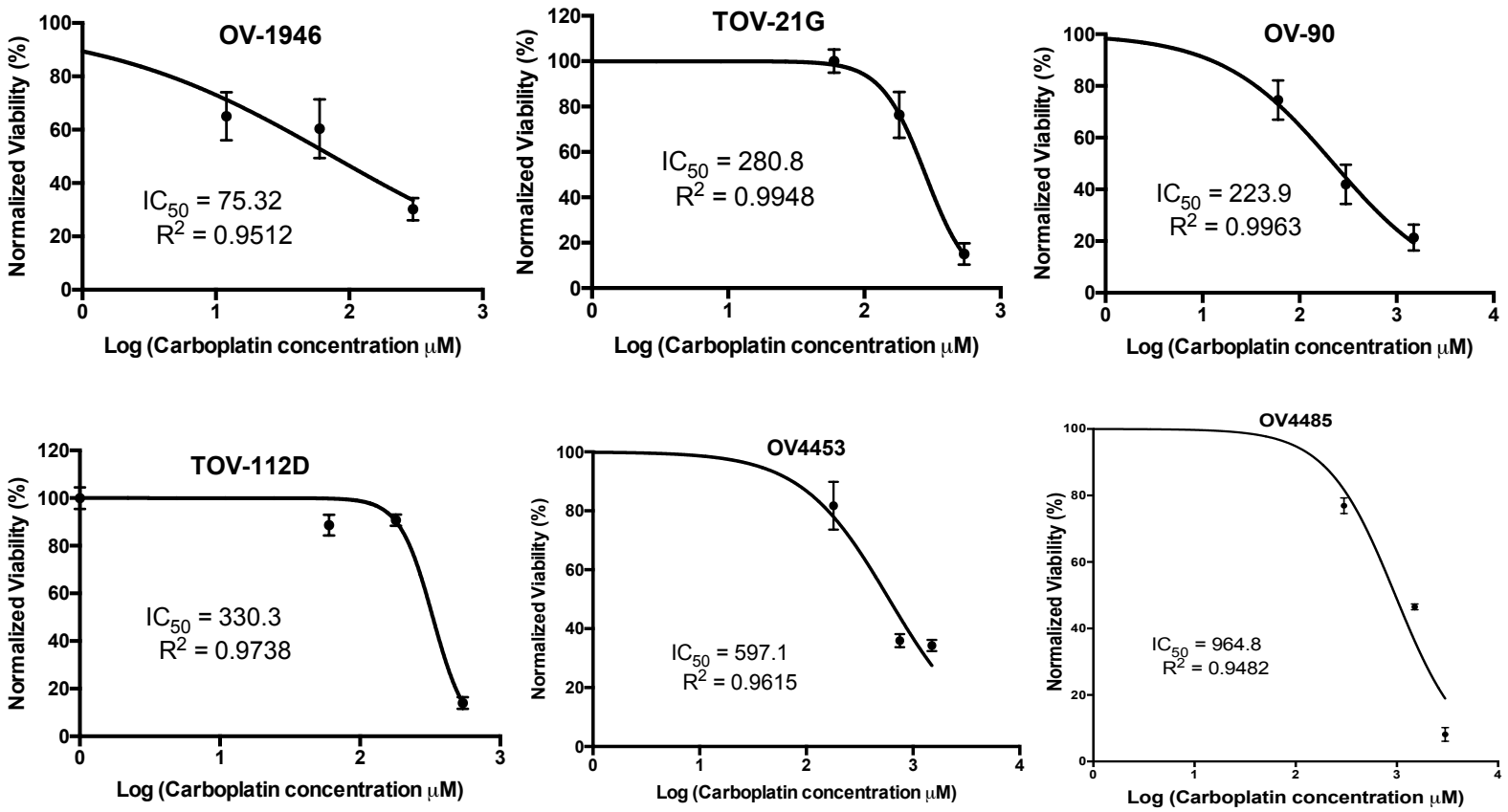

Figure 3. **Carboplatin chemosensitivity in 3D spheroid models for all 6 EOC cell lines**

A) Spheroid cell viability (normalized to Control) with three different carboplatin doses (24-hour treatments) B) Dose-response inhibition curves (in order of ascending IC_{50}). All experiments were performed at least three times (range, 3-6). IC_{50} in μM. Error bar = ± SEM. *p<0.05, **p<0.01, ***p<0.001, ****p<0.0001

Table 4. **Carboplatin IC_{50} fold change between 2D and 3D models. IC_{50} in μM**

Cell Line	**3D IC_{50}/2D IC_{50}**
OV4453	659.1/0.23 = 2865.7
TOV-21G	280.8/1= 280.8
OV-1946	90.03/3.4 = 26.5
OV4485	964.8/6.1 = 158.2
TOV-112D	330.3/13.4 = 24.7
OV-90	223.9/31.8 = 7.0

In vivo Xenograft Mouse Model

Tumor volume curves were generated from recorded xenograft measurements throughout carboplatin treatment (Figure 4). Chemosensitivity was categorized according to the ability of each cell line to inhibit *in vivo* tumor growth. As such, a cell line was considered resistant if no statistical difference was seen with even the highest dose (unresponsive), sensitive when tumor volumes at time of sacrifice were significantly lower than the controls for at least the two highest carboplatin doses used (very responsive), and intermediate for responses that were incomplete (partially responsive). Therefore OV-1946 and OV4453 were categorized as sensitive, OV-90 and OV4485 as intermediate, and TOV-21G and TOV-112D as resistant. As seen with the 3D model, chemosensitivity varied significantly in the xenograft model when compared to the 2D-determined ranking.

A)

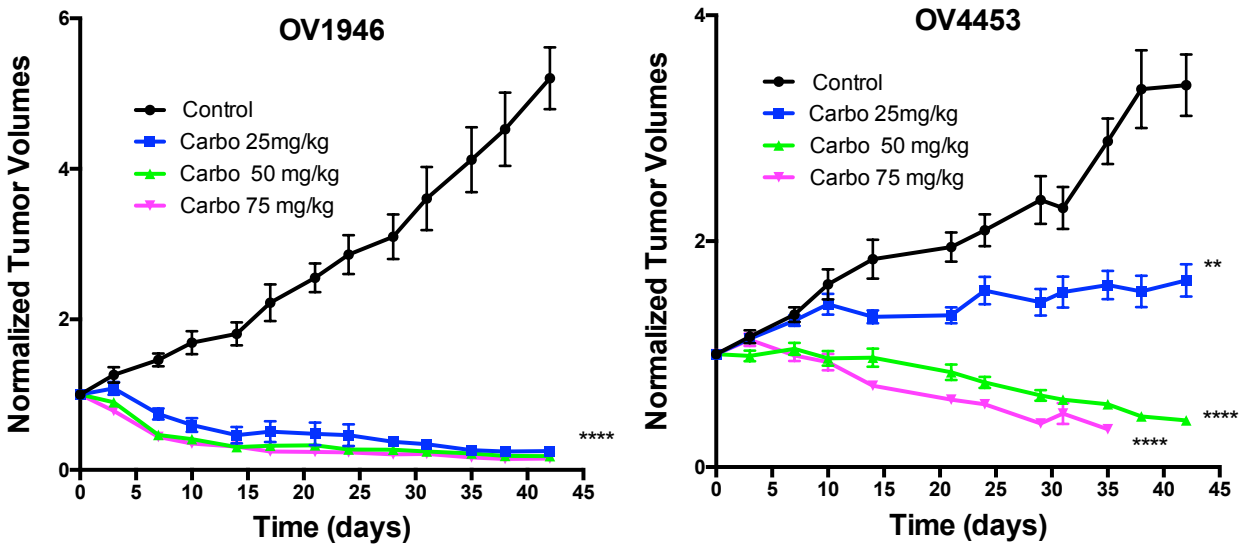
OV1946
Normalized Tumor Volumes
Time (days)
Control
Carbo 25mg/kg
Carbo 50 mg/kg
Carbo 75 mg/kg
****
OV4453
Normalized Tumor Volumes
Time (days)
Control
Carbo 25mg/kg
Carbo 50 mg/kg
Carbo 75 mg/kg
**
****
****

B)

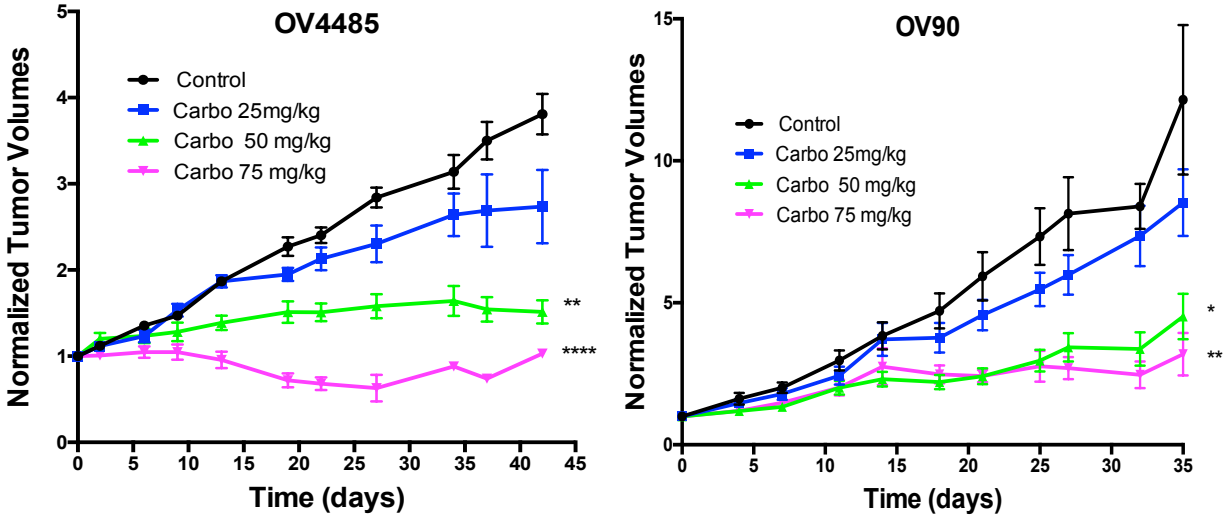
OV4485
Normalized Tumor Volumes
Time (days)
Control
Carbo 25mg/kg
Carbo 50 mg/kg
Carbo 75 mg/kg
**
****
OV90
Normalized Tumor Volumes
Time (days)
Control
Carbo 25mg/kg
Carbo 50 mg/kg
Carbo 75 mg/kg
*
**

C)

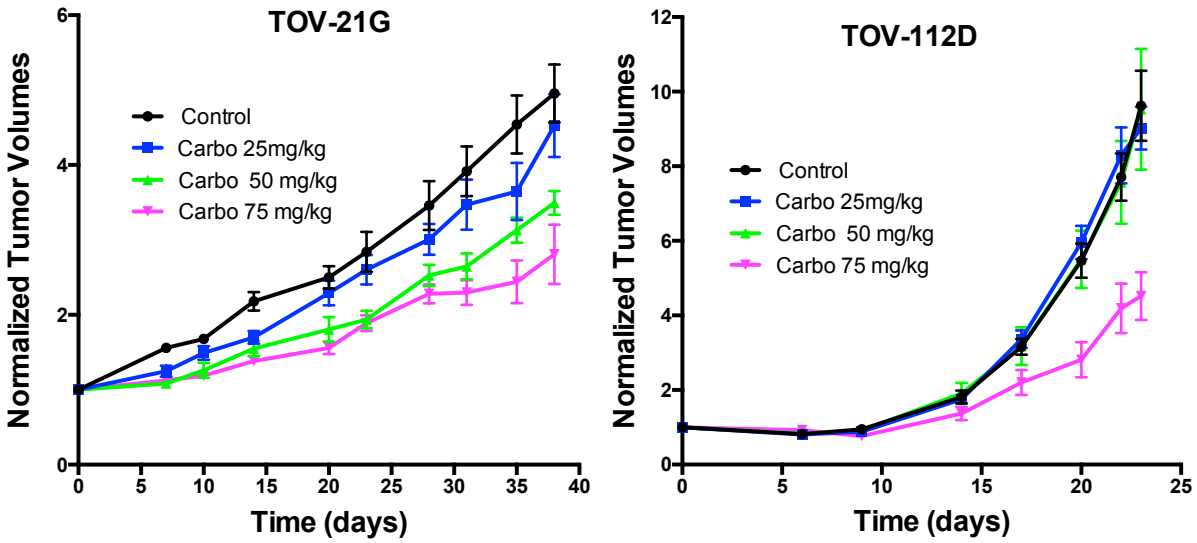

Figure 4. **Quantitative analyses of epithelial ovarian cancer growths in mouse xenografts**

Weekly IP treatments were administered up to a maximum of 6 cycles (8 mice/condition) were started once tumor was >200mm^3. Treatment groups included control (0.9% NaCl), 25mg/kg, 50 mg/kg and 75 mg/kg of carboplatin). Average growth curves of tumor volumes were plotted over time. The cell lines were then classified based on treatment-response: the two most sensitive cell lines OV-1946 and OV4453 (A), the two intermediate cell lines OV4485 and OV-90 (B), and the two most resistant cell lines TOV-21G and TOV-112D (C). Black line = Control, Blue line = Carboplatin 25 mg/kg, Green line = Carboplatin 50 mg/kg, Pink line = Carboplatin 75 mg/kg. Normalized values were obtained by calculating the volume at any given time (T_x)/ volume at Day 0 (T_0). Error bar = ± SEM

Quantitative IF was generated from the collected xenografts after carboplatin treatment completion. IF staining with Ki-67 antibody showed a significant decrease in proliferative cells after treatment (Figure 5). The response was dose- and cell-line dependent and EOC cell lines were subsequently categorized according to chemosensitivity. TOV-112D and TOV-21G were resistant across all doses. OV-1946 and OV4453 had a very significant response ($p<0.001$) with the two highest doses compared to control, making them sensitive cell lines. OV-90 and OV4485 demonstrated partial response and was therefore classified as intermediate. These results are concordant with the tumor volume measurements.

A)

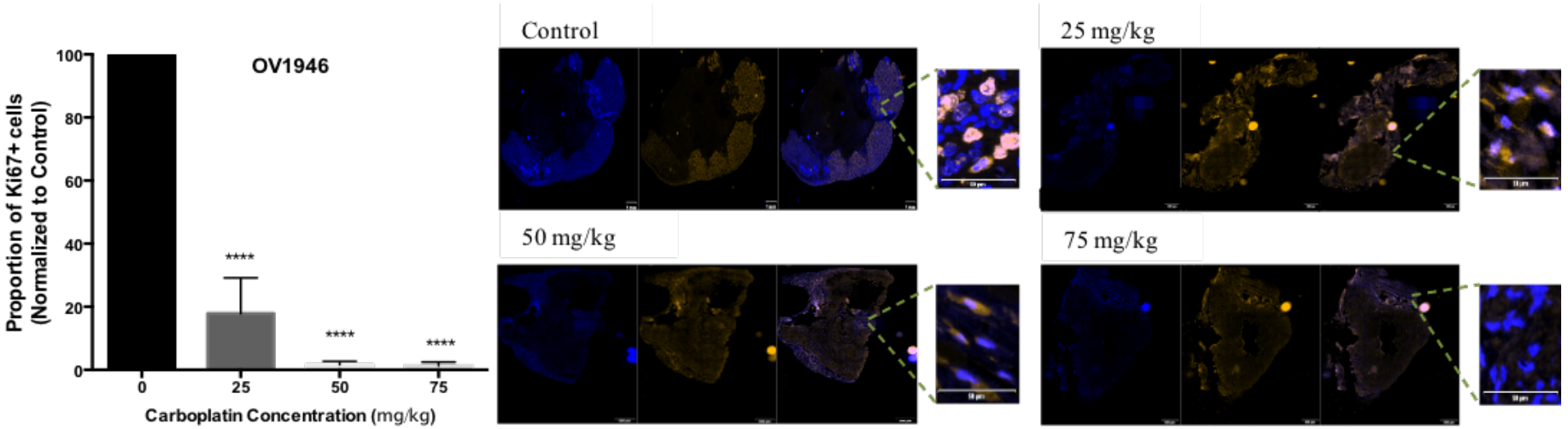
OV1946
Proportion of Ki67+ cells (Normalized to Control)
100
80
60
40
20
0
****
****
****
0
25
50
75
Carboplatin Concentration (mg/kg)
Control
25 mg/kg
50 mg/kg
75 mg/kg

B)

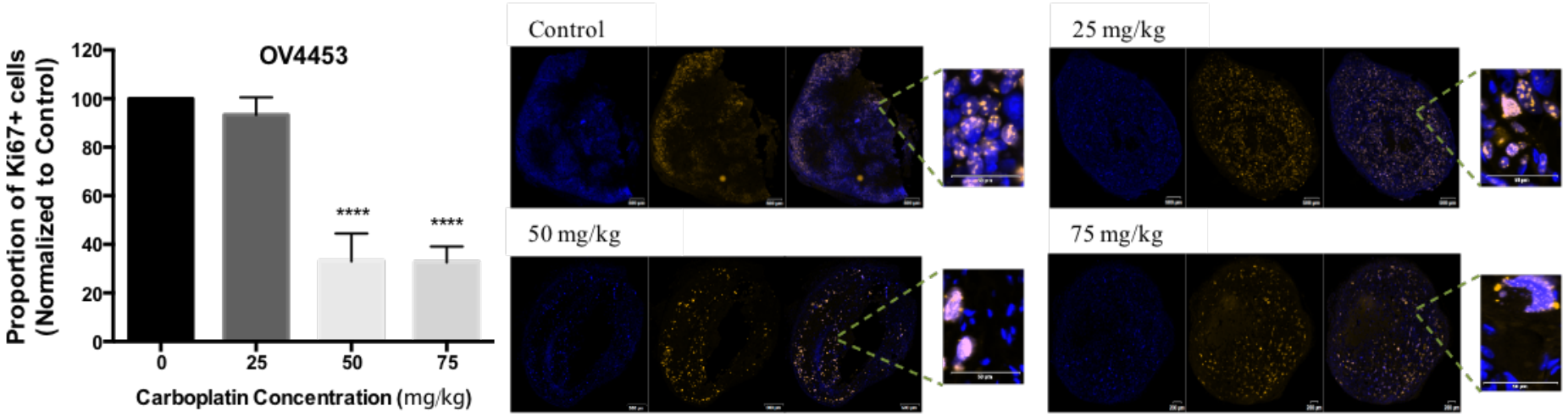
OV4453
Proportion of Ki67+ cells (Normalized to Control)
120
100
80
60
40
20
0
****
****
0
25
50
75
Carboplatin Concentration (mg/kg)
Control
25 mg/kg
50 mg/kg
75 mg/kg

C)

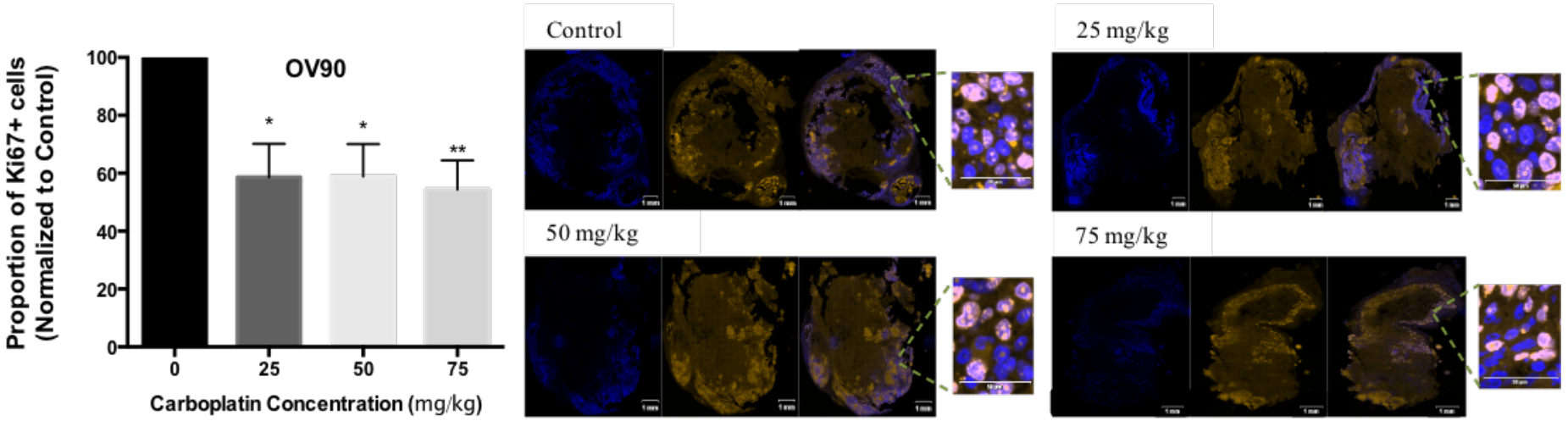
OV90
Proportion of Ki67+ cells (Normalized to Control)
100
80
60
40
20
0
*
*
**
0
25
50
75
Carboplatin Concentration (mg/kg)
Control
25 mg/kg
50 mg/kg
75 mg/kg

D)

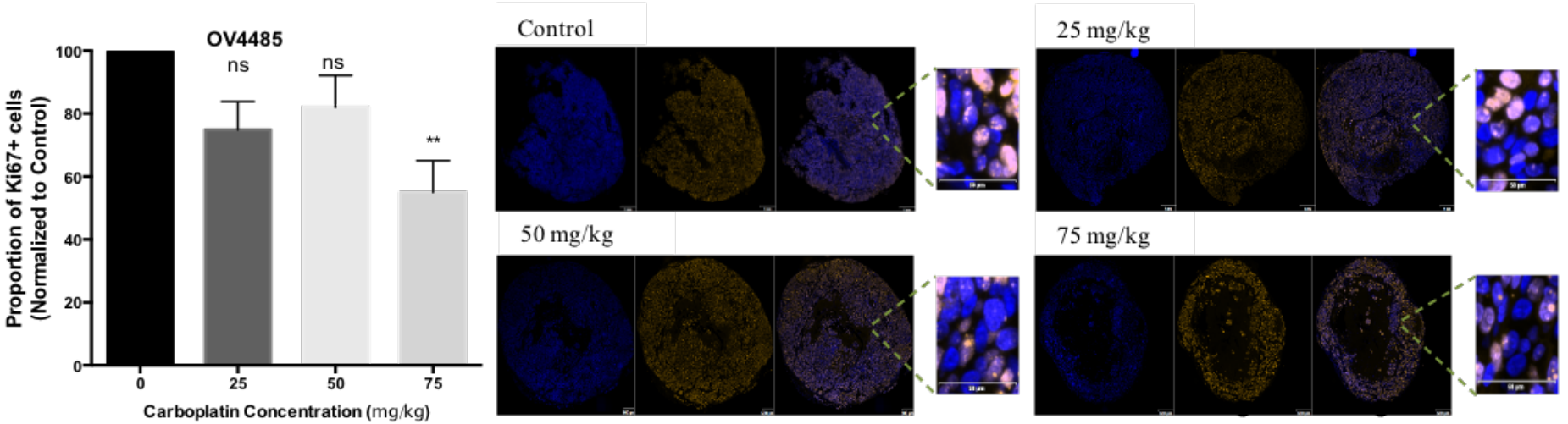
OV4485
Proportion of Ki67+ cells (Normalized to Control)
100
80
60
40
20
0
ns
ns
**
0
25
50
75
Carboplatin Concentration (mg/kg)
Control
25 mg/kg
50 mg/kg
75 mg/kg

E)

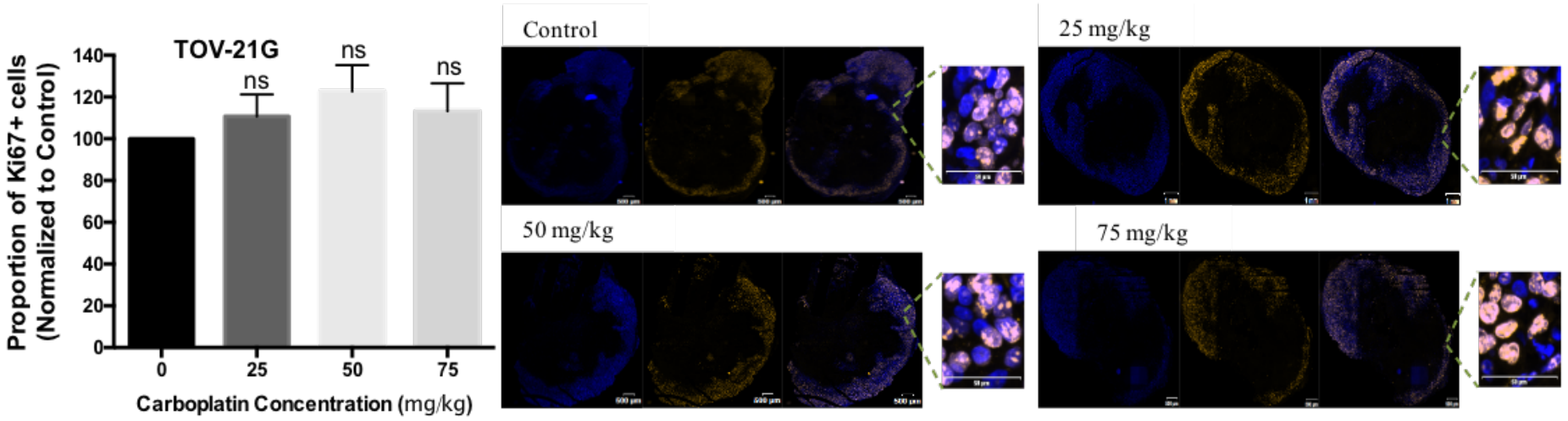
TOV-21G
Proportion of Ki67+ cells (Normalized to Control)
140
120
100
80
60
40
20
0
ns
ns
ns
0
25
50
75
Carboplatin Concentration (mg/kg)
Control
25 mg/kg
50 mg/kg
75 mg/kg

F)

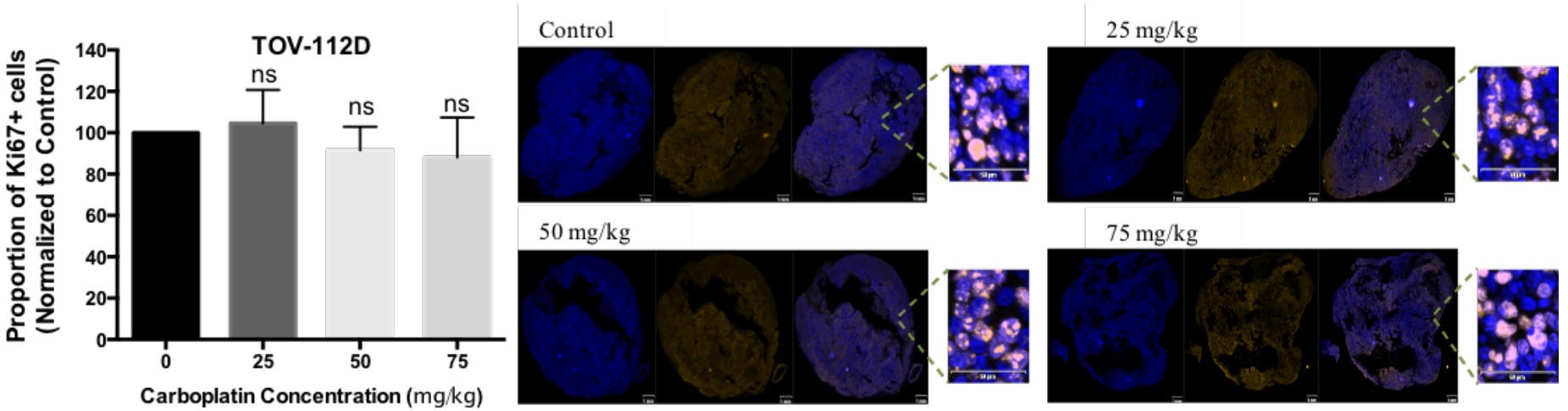
TOV-112D
Proportion of Ki67+ cells (Normalized to Control)
140
120
100
80
60
40
20
0
ns
ns
ns
0
25
50
75
Carboplatin Concentration (mg/kg)
Control
25 mg/kg
50 mg/kg
75 mg/kg

Figure 5. **Dose-response analysis of EOC cell line xenografts.**

Mice were treated with 3 concentrations (25, 50 and 75 mg/kg) of carboplatin. Xenografts were formalin-fixed and paraffin-embedded. IF staining of xenografts (DAPI in blue, Ki-67 in yellow) and quantification were performed for all 6 cell lines (n= 8 mice/condition) A) OV-1946 B) OV4453 C) OV-90 D) OV4485 E) TOV-21G F) TOV-112D. Normalized values were obtained by calculating the viability at a given carboplatin concentration (Cx)/viability of the control group in percentage for each experiment. Error bar = ± SEM

Comparing 2D, 3D and *in vivo* Carboplatin Sensitivity

When trying to correlate the *in vivo* chemosensitivities with that of the *in vitro* models, results appeared to vary according to the cell line. We found that the *in vivo* results of the cell lines OV4453 and OV4485 resembled the 2D chemosensitivities more than the 3D spheroid model did. Conversely, the *in vivo* chemosensitivity of cell lines OV-1946 and OV-90 were better reflected in the 3D spheroid model. TOV-112D *in vivo* response reflected both 2D and 3D response. TOV-21G showed different rankings across the 3 different models, however both 3D spheroid and *in vivo* responses were more resistant than the 2D model (Table 5). In summary, we observed that carboplatin responses of 3D-spheroids resembled that of the *in vivo* model in 4/6 cell lines, while two cell lines (OV4453 and OV4485) did not. These two cell lines were the most resistant in the spheroid model.

Table 5. **Summary of chemosensitivity across model systems.**

Cell lines	**2D**	**3D**	**Xenograft**	***In vivo* correlation**
OV4453	Sensitive	Resistant	Sensitive	**2D**
TOV-21G	Sensitive	Intermediate	Resistant	**-**
OV-1946	Intermediate	Sensitive	Sensitive	**3D**
OV4485	Intermediate	Resistant	Intermediate	**2D**
TOV-112D	Resistant	Resistant	Resistant	**2D + 3D**
OV-90	Resistant	Intermediate	Intermediate	**3D**

Chapter 4 – Discussion

This study highlights the importance of preclinical model selection for drug sensitivity analysis and understanding the variation that exists between experimental models. As most early-phase clinical trial designs rely heavily on preclinical data, it is important to consider these findings when performing drug screening or therapeutic response prediction studies especially in the era of personalized medicine. Given the major patient burden and cost of trials to our health care system and limited funding available, we must improve the high attrition rates of anti-cancer drugs making its way to the clinic, and this begins with understanding the current models we have available today to identify areas of improvement.

The mainstay of preclinical studies still remains cell-line based experiments. Few studies have reported results for chemosensitivity in the same patient-derived cell lines across 2D, 3D and animal models. An older study by *Erlichman et al* used bladder carcinoma cells and reported that the 3D *in vitro* model reflected better the response found in their mouse xenograft model, and higher drug resistance was seen in 3D compared to 2D culture [68]. In our study, the more representative *in vitro* model varied according to cell line. However, the majority of the cell lines showed better concordance in carboplatin sensitivity between 3D spheroids and *in vivo* responses. When comparing 2D and *in vivo* models, many interesting observations can be made. Namely that certain cell lines that have been traditionally characterized in 2D and labelled as sensitive, such as TOV-21G, can be completely resistant when therapeutic response is tested *in vivo*. Conversely, one of the most resistant HGS ovarian cancer cell lines in our laboratory's panel of EOC cell lines, OV-90, becomes much more sensitive when platinum therapy is tested in mouse models. The transition from 2D to 3D, in our study, also displayed an increase in resistance,

however not all to the same degree, which accounted for the rank order changes amongst the 6 cell lines. Understanding how cancer cell lines behave across model systems is crucial so as to not under- or over-estimate drug response.

The differences seen across model systems may be due to multiple factors, including but not limited to origin of cell line (location, histology and previous treatments), morphology, drug penetration[106], changes in protein expression, hypoxia, stemness, and the type of drug tested. A more detailed discussion of these factors is considered in the following sections. These factors will likely influence the choice of model system when developing therapeutics.

Factors Influencing Drug Response in Ovarian Cancer Preclinical Models

Origin of cell line impacts preclinical therapeutic responses

For proper model selection and interpretation of responses observed in the model, it is important to know where the cells used are derived from. In the case of immortalized human cancer cell lines, this requires a comprehensive understanding of the original patient's disease. It has been reported that cell lines derived from previously treated tumor or ascites often develop acquired platinum resistance[102]. This is likely due to protein expression changes (e.g., loss of luminal cytokeratin (CK) 8/18/19)[102] or new mutation profiles that are acquired after exposure to treatment. From these cell lines only OV4485 was derived at time of recurrence[99], which could explain its higher resistance to carboplatin in 3D spheroids. In addition, location of derived cell is equally important. A study performed by *Mo et al*[109] using a tumor-derived ovarian cancer cell line as well as ascites derived from *in vivo* culture of this same cell line demonstrated that the

cells from ascites and cells cultured with ascites medium had increased 2D chemotherapy resistance compared to that in the original cancer cell line culture. The ascites culture also showed evidence of increased drug efflux and an increase in multidrug resistant ATP-binding cassette (ABC) transporters. However, such a correlation with carboplatin sensitivity could not be observed in our study, where the four cell lines derived from ascites samples (OVs) presented variable carboplatin responses in all three models used. The two cell lines derived from tumor samples (TOVs) were the most resistant in the *in vivo* model. However, it is important to mention that these two TOV cell lines are derived from rarer EOC subtypes, clear cell (TOV-21G) and endometrioid (TOV-112D), known to be more chemoresistant than the HGS histology[58]. This is likely a result of the distinct genetic mutation profile that characterizes them. With the advent of tumor molecular characterization, this will further increase our understanding of EOC subtypes, and it becomes even more important to appropriately select a model that best addresses a given research question.

Impact of hypoxia on drug response

Inherently, *in vivo* models exhibit chemical gradients (e.g., nutrients and oxygen), and by extension biological changes (gene/protein expression), that define their TME. 3D models such as spheroids attempt to mimic this gradient, while this is quasi absent in 2D models.

Cells in a 3D spheroid demonstrate lower viability than cells plated in a 2D culture. *Shan et al* demonstrated that, without any cytotoxic treatment, a 40% decreased viability is noted in cells of a spheroid (5000 cells) compared to its monolayer model[90]. Similar to our results, *Rosso et al* found that OV-90 cells had twice as many dead cells than TOV-112D cells after 48 hours of formation (without drug treatment) simply by culturing in aggregates instead of monolayers[110].

Another study in breast cancer cell lines showed an increase in the proportion of necrotic and apoptotic cells in 3D compared to 2D, and this effect was more important as the size of the spheroid increased (more initial cell seeding)[79].

Morphology and viability of cells in a model system will inevitably affect drug penetration. *Shan et al* performed pharmacological assays that detected lower fluorescent drug intensities in the inner cores of spheroids compared to the outer proliferative layer. These central drug intensity values decreased with increasing cell seeding number and spheroid size[90]. For the same drug tested, this effect was similarly seen with increased IC_{50} values reported. This may be in part related to the hypoxic core that develops in a spheroid as it increases in size (gradually seen as spheroids exceed 200-500μm)[71 77 79]. Many spheroids in human ascitic fluid appear to exceed this size and thus likely exhibit this feature[71]. *Gong et al* showed a 50 to 80 fold difference in IC_{50} values using doxorubicin in breast cancer cell lines; as the size of the spheroid increased, drug penetration decreased and resistance increased[79]. Our group had previously found a 9-fold increase in IC_{50} for the cell line TOV-112D spheroids obtained with the hanging droplet technique[95] and an 18-fold increase using the non-adherent plate technique[83]. Spheroid diameters were no larger than 200μm[95] and 300-400μm, respectively[83]. Furthermore, model systems that inherently demonstrate evidence of hypoxia can be expected to incur changes in gene/protein expression compared to models, such as monolayers, that do not. The changes in cell gene and protein expression within spheroids such as increased markers of stemness (CD44) and angiogenesis (VEGF) due to hypoxia may contribute to the chemoresistance seen in 3D models[79]. In this context, it is possible that the high carboplatin resistance of OV4453 and OV4485 spheroids might be related to their low oxygen supply. These were the only two cell lines in our study in which spheroids were cultured in low oxygen (7%) conditions. These cell lines are

sensitive to oxygen and they grow slower in normal 21% oxygen. Nevertheless, this low oxygen condition does not affect 2D response, as OV4453 is one of the most sensitive cell lines to carboplatin (evaluated by clonogenic assay)[99]. Furthermore, *Hirst et al* demonstrated an increase in hypoxia-regulated genes (presence of HIFα) and markers of stemness with negative staining for Ki-67 in the core of 3D multicellular tumor spheroids which was not seen in monolayers[111]. The results argue that chemoresistance and increased stemness may not simply be due to poor drug penetration alone, but rather related to phenotypic changes of cells in 3D that persist even when dissociated into single-cell suspension[111]. *Muñoz-Galván et al* reported differences in 3D gene expression profiles for cancer stem cell (CSC)-related genes that were overall significantly higher compared to 2D profiles. Furthermore, when analyzing sensitive and resistant tumor samples, CSC-related genes were also significantly higher in the resistant cohort. Inhibition of some of these CSC markers in combination sensitized the cells to even low doses of carboplatin as shown by decreased ability to form spheroid[112]. Taken together, it is important to consider the hypoxic changes that occur in more complex model systems and how this impacts response to therapy.

Impact of EMT and DNA repair on drug response

To account for biological and therapeutic response differences of cancer cell lines across different model systems, cell adhesion markers may be important in different culture settings and DNA repair mechanisms appear to vary across cell lines and experimental models.

EMT markers have been studied for correlation with chemoresponse and, in the case of 3D spheroids, morphology without any convincing trends. Within the panel of EOC cell lines in our study, we were not able to find a correlation between therapeutic response and EMT markers. For

TOV-21G, the original 2D characterization of the cell line demonstrated positive CK 8/18/19 protein on IF[101] while a more recent publication using FACS analysis failed to detect the same CKs and epithelial cell adhesion molecule (EpCAM) expression[102]. VIM expression (2D-cell pellets) was found to be positive in TOV-21G using IHC[113]. TOV-112D similarly had positive CK 8/18/19 on the original 2D characterization of the cell line[101], however other recent analyses demonstrate negative expression of PAN-CKs, ECAD and/or EpCAM (Western blot, FACS or IF)[102 110]. VIM was found to be positive (IHC or Western blot)[110 113]. Put together, these would suggest that TOV-21G and TOV-112D have a more mesenchymal type of phenotype, however the results are nevertheless ambiguous. OV-90 monolayer cells express CKs 8/18/19 and PAN-CKs, EpCAM and ECAD[101 102 110] but not VIM[110 113] suggesting a more epithelial phenotype. Both TOV-112D and OV-90 cell lines were also evaluated for EMT markers when cultured as 3D spheroids and the protein expressions did not change significantly[110]. OV-1946 does not express epithelial markers CKs 7/8/18[100] and ECAD[114] suggesting a more mesenchymal phenotype. 2D characterization of the OV4453 and OV4485 cell lines show that both express CKs 7/8/18/19 but not VIM, and only OV4485 expresses ECAD[99]. Altogether OV4453 and OV4485 appear to express markers from both epithelial and mesenchymal phenotypes suggesting an intermediate phenotype. In summary, when evaluating these markers and phenotypes in our panel of 6 EOC cell lines, no clear trend could be established with either *in vitro* or *in vivo* therapeutic response, further stressing the need to test in different models.

Other studies have looked at the association of response and morphology, and changes in these markers when culturing in 2D and 3D. *Heredia-Soto et al* evaluated protein expression (through IHC) of markers SNAIL, SLUG, ZEB1, ZEB2, TWIST1, TWIST2, ECAD, PANCK, NCAD and VIM between 2D and 3D cultures. Although a general increase in EMT markers expressed was

noted in the 3D culture, unfortunately no correlation could be made with phenotype and response to platinum therapy[115]. Similar studies using our EOC cell lines TOV-21G, TOV-112D and OV-90 did not find any significant changes in some of these markers from 2D to 3D[88 110], however one study suggested a trend towards epithelial phenotype transition in 3D culture[88] but this was in contrast to other published studies[115]. Furthermore, when attempting to correlate EMT phenotype and spheroid morphology, no clear trend could be established for compact or loose aggregates[88].

Besides EMT markers, differences in DNA repair capabilities (related to DNA mutation or methylation) across cell lines may play a role in therapeutic response, particularly platinum-therapy. There are 3 DNA repair mechanisms relevant to the EOC cell lines used in this study: homologous recombination (HR), non-homologous end-joining (NHEJ), and MMR deficiency. In the case of the cell line OV-90, the observed carboplatin sensitivity in 3D and *in vivo* models compared to the 2D model may be explained by reported lowered levels of BRCA 1 protein and a mutation in the *XRCC5* gene, which codes for a protein required for NHEJ repair of DNA double strand breaks, suggesting a dysregulation in DNA repair mechanisms in this cell line compared to other BRCA wildtype cell lines[116]. Interestingly, in a study treating OV-90 cells with the PARPi, olaparib, a significant decrease in IC_{50} was noted when cells were cultured in 3D spheroids compared to monolayers[82]. Moreover, as previously mentioned, both OV4453 and OV4485 cell lines are BRCA deficient hence with impaired HR. HR deficient cells are often more susceptible to DNA alkylating agents such as carboplatin which correlates with the response observed *in vivo*. Moreover, loss of function (gene mutation or methylation) of the MMR proteins that repair single base mismatches and insertion/deletion loops can create DNA damage tolerance[117 118]. This deficiency was noted in the cell line TOV-21G[101] which may confer its significant chemoresistance in xenograft models and in spheroids. There are several reported causes of this

increased chemoresistance in MMR deficient tumors the main mechanism being that DNA damage detection and subsequent downstream activation of cell death are impaired[119]. However, it remains a mystery why TOV-21G is consistently sensitive in 2D models and may reflect some of the shortcomings of 2D models that do not account for the TME, chemical gradients and cell interactions that are present in 3D and *in vivo* models. Furthermore, given some of these biological changes that appear to occur when cells are culture in 2D versus 3D, it may not come as a surprise that some studies report different xenograft tumor growth/tumorigenicity[120] and angiogenesis[121] when cells are cultured in 3D prior to injection in mice. Interestingly, when OV-90 xenografts were established from monolayers versus spheroids, the tumor growth was no faster when derived from the 3D than the 2D model, which is consistent with our findings[86]. Overall, it appears that EMT and DNA repair markers influence drug response, however further studies across different model system are required to understand their predictive value in determining drug sensitivity.

Factors that influence drug penetration relevant to in vitro therapeutic response

With different *in vitro* culture methods, it would be expected that *in vitro* drug penetration, and hence drug sensitivity, would vary according to morphology, drug exposure time, drug molecular weight and mechanisms of drug accumulation/inactivation.

In trying to correlate morphology and drug response, *Lee et al* discovered increased resistance in 3D EOC models compared to their 2D counterpart with the greatest change in sensitivity amongst cell lines forming large dense and large loose aggregates[88]. This finding could account for the higher platinum-sensitivity seen in the two cell lines forming the small compact spheroids in our work, OV-1946 and OV-90. Another study using a breast cancer cell line compared 3D spheroid

model and a 3D microtissue model and found decreased drug penetration in spheroids compared to the microtissues, and one potential hypothesis they reported was that the spheroids were more compact[122].

Drug exposure time may also influence the ability for drugs to penetrate *in vitro* models and thus drug response. *Shan et al* studied three different drug exposure times at 1 hour, 24 hours and 72 hours with ellipticine and doxorubicin. At 1-hour, cytotoxic drugs accumulate in the outer layer, and only after 24 hours exposure do the spheroids start to demonstrate evidence of disintegration with a decrease in drug intensity differential between outer and inner cell layers. This indicates improved drug penetration. 72 hours of exposure to high dose cytotoxic drug induced apoptosis in cells of spheroids[90].

Some of these variations in therapeutic response may be due to the molecular weight of the agents tested, with low-molecular weight drugs penetrating more easily[106]. Although most patients receive combination treatment of carboplatin and paclitaxel in the first line setting, we chose to treat solely with carboplatin. As previously mentioned, carboplatin response, and not paclitaxel, is a biomarker for response to second-line therapy. Furthermore, paclitaxel's effect (IC_{50}) does not appear to vary significantly across our EOC cell lines[123].

Drug penetration and chemosensitivity can also be influenced by differences in gene and protein expression across different models and cell lines[117]. Platinum resistance may be related to protein changes that result in reduced intracellular drug accumulation, namely through decreased drug influx or increased drug efflux. ABC transporters/pumps are the main players in multidrug resistance by exporting cytotoxic drugs from the cell. The well-known ABC transporters involved in platinum resistance are MRP2, CTR1 (a copper transporter) and ATP7A/B (copper exporters)[124 125]. ATP7A also may sequester platinum agents in intracellular compartments before

attaining nuclear DNA[117]. Furthermore, the glycoprotein drug transporter, P-glycoprotein, is also an efflux pump that has been associated to platinum resistance *in vitro* and *in vivo* and whose expression increases in the presence of drug[117 118]. Lung resistance protein (LRP) is a nuclear extrusion transporter of molecules between the nucleus and cytoplasm and their exocytosis from the cell[118]. Proteins involved in drug efflux may be upregulated in some cells located in the core of the spheroid with evidence of inactive metabolite in this region of the spheroid[74 80] resulting in lower 3D chemosensitivity that correlated with results from *in vivo* studies[74]. Other mechanisms of platinum resistance are related to intracellular drug inactivation through upregulation of detoxification enzymes. In the cytoplasm, platinum drugs undergo aquation allowing them to react with thiol containing molecules, such as glutathione that sequesters the drug reducing oxidative stress and allowing DNA repair[118 124]. In response to hypoxia for example, activation of the oxidative stress response (Nrf2 pathway) increases the enzyme that synthesized glutathione[126]. Another detoxifying enzyme, aldehyde dehydrogenase (ALDH), oxidizes aldehydes to weak carboxylic acids and increased expression has been noted in resistance cells and is a known marker of ovarian cancer stem cells. 3D spheroids express higher levels of ALDH[127]. To our knowledge, no studies have evaluated the expression of these transporters or enzymes in our panel of EOC cell lines and should be evaluated in future studies.

The ability for a drug to interact with the cells in a model is influenced by many of these factors and should be taken into account during the study design phase.

How a drug and its therapeutic analysis method may influence drug response

The differences in response across models vary according to the mechanism of action of a therapeutic agent tested. In the case of targeted therapy, the trends in model systems appear to different depending on the agent[76]. As an example, glioblastoma cell lines were more sensitive

with targeted therapy PI3 kinase inhibitor in a 3D model compared to 2D monolayer culture[81]. However, when exposed to other targeted therapies such as HSP90 chaperone or PLCγ inhibitors, the 3D cultured cells were more resistant than in monolayers.

In comparison with cytotoxic chemotherapy, generally cells become more resistant in 3D although to variable degrees[12], as we have seen in our study with carboplatin. In addition, the 3D/2D growth inhibition ratio (GI_{50}) can vary significantly depending on the agent and the cell line used. *Shan et al* reported ratios that were 6 to 20-fold higher when testing plant alkaloid or anthracyclines chemotherapeutics[90] and another study described an increase of 2 to 5 fold concentration to inhibit 50% of cell growth with 5-fluorouracil, paclitaxel or curcumin[128]. *Heredia-Soto et al* treated a panel of EOC cell lines with cisplatin in 2D and 3D cultures only up to a maximum of 100μM. IC_{50}s performed for all cell lines in 2D and 3D (with some unable to be reached) demonstrated a range of 5 to more than 50 fold difference in chemoresistance[115].

It is important to consider that some of the differences seen may be related to the analysis method chosen to evaluate drug response to therapy. One of the important elements of a useful preclinical drug discovery model is its ability to perform HTS. To this end, treatment response is often determined through colorimetric/fluorimetric assays such as MTT[128] to indirectly determine cell viability. However, these analytical tests that rely on metabolic state of cells often overestimate viability when compared to growth-inhibition or clonogenic assays. This is seen in particular with drug- or radiation-induced senescence[129]. For this reason, we chose to use LIVE-DEAD FACS stain to analyze the chemosensitivity in our 3D model, although not a high-throughput assay. However, flow cytometry may limit the number of concentrations tested and hence may give less accurate assessment of IC_{50} values generated. One method that allows HTS and has been used by others is the image cytometer[81 115] which can quantify fluorescence in a 3D model without

needing to dissociate the cells for flow-based analysis. Therefore, additional elements such as morphology and localization that may allow to better understand a phenotype. Furthermore, to ensure both quantitative and qualitative therapeutic assessment of our xenograft model, we used both tumor volume as well as protein immunofluorescence viability testing. Both provided similar findings supporting our conclusions. In summary, one must consider the drug being tested in a given model as well as the assay used to determine therapeutic response

Moving to more complex model systems

Complex 3D models

To circumvent some of the shortcomings of monolayer cultures, and more simple 3D models such as spheroids, new complex *in vitro* models are being developed. Patient-derived organoids (PDO) has emerged as a new model that could offer the ease of HTS and better approximation of the TME (morphology, mutation profile, gene expression patterns)[130 131]. These PDOs are generated through digestion of original tumor and are often associated with an embedded ECM. Organoids are 3D clusters of cells derived from pluripotent stem cells that differentiate into a structure with multiple cell types to mimic the original tumor specimen[131 132]. This model has been explored in normal tissue such as fallopian tube and multiple cancers such as ovarian, breast, colon, endometrium with high success over short-term[131] and long-term culture[133 134]. This could allow the inclusion of the ultimate control assay by including effects on normal tissue. Trials are underway to verify if PDOs correlate with patient response[135 136]. Organoids can also be a good model to study biomarkers. 3D co-culturing can improve modeling by re-establishing cell interactions and signaling[80]. *Jabs et al* demonstrated varied responses across a panel of 22 drugs or combinations, including carboplatin, in 2D monolayer and 3D organoid culture[130]. Some studies have looked at incorporating an element of fluid shear stress to mimic the transcoelomic

metastases of EOC[137]. Furthermore, organoids can also be derived from xenografts (called PDX-O)[134].

Studying stem cells that represent a minor portion of tumor cells can be challenging without requiring a large quantity of starting tissue material. *Raghavan et al* developed a spheroid model that requires no more than 100 cells to generate spheroids, which make studying EOC stem cells more convenient[94]. Likewise, *ex-vivo* micro-dissected tumors in microfluidics devices and cancer tissue explants are also emerging as a viable model for drug prediction[31 108 138]. We are the pioneers of this technology which we plan to incorporate in our comparative analysis in the future (see Perspectives section).

Complex In Vivo Models

More complex *in vivo* models have been developed recently as well to improve preclinical testing, namely PDXs. Patient tissues are engrafted in immunocompromised mice and can be passaged and cryopreserved while maintaining most of the original tumor characteristics[12 59 62]. Preliminary studies show that the PDX response closely resembles the patient clinical response[12]. Until the time and costs to establish these models decreases, it may be less useful as a new drug discovery tool, but rather serve as a useful drug response and biomarker identification model or patient avatar screening model[12 59 134]. Whether the murine stromal replacement that occurs with subsequent passaging of PDXs is of concern is still being studied[12]. As well, lack of a murine immune system limits its use to study the impact of the immune response to cytotoxic, targeted therapy or immunotherapy[12]. Humanization of mice through peripheral blood mononuclear cell (PBMC) or CD34+ (hematopoietic progenitor cells) cell injections may mitigate some of these shortcomings[139]. To add to the growing body of knowledge of immuno-oncology, the

microbiome has emerged as a potential biomarker for therapeutic response through its effect on the immune system. In lung cancer, the gut microbiota has been correlated to response rates, survival and adverse events after immune checkpoint inhibition treatment[140]. This will likely need to be incorporate in mouse models, especially if immunotherapy is included in the treatment combination. Investing upfront in more reliable and accurate preclinical models will likely save more money in the drug discovery pipeline[96] because of higher quality leads that are translatable in the clinic[57].

Challenges of Preclinical Models

The potential concerns with cell line-based models

The greatest challenge for scientists in the field of drug discovery is to identify the right *in vitro* model that will reproduce *in vivo* results. Drug discovery still relies heavily on cell line-based studies but has received many criticisms. *Gillet et al*[141] studied the multidrug resistance transcriptome, using the NCI-60 panel, of cancer cell lines cultured in different model systems (2D monolayers, 3D spheroid, mouse xenograft model). They reported an upregulation of pro-survival genes in cancer cell lines compared to treatment naïve primary clinical samples. However, when a panel of multidrug resistance (MDR) genes were evaluated in both groups, they could not find a correlation between expression profiles. In fact, results across different model systems from one ovarian cancer cell line most closely resemble each other and not the clinical tumor samples. Based on these findings, they put into question the validity of studying aspects of cancer biology and therapeutic response (mechanism or modulation of clinical drug resistance) using cancer cell lines. However, the NCI-60 panel does not include any EOC cell lines derived from our laboratory that have been extensively characterized. Potential reasons for these observed differences are described below.

The challenges with traditional in vitro models

As previously mentioned, there exists multiple technique for spheroid generation. Not all spheroid generation techniques are equivalent. It has also been studied that different spheroid formation methods can lead to different expression profiles of cell-cell and cell-matrix interactions as well as different drug sensitivities[75 142]. For example, one study showed that hanging droplet technique generated more ECM deposition and incurred more resistance than ULA plates[142]. Furthermore, drug sensitivities can depend on the cell line used as well[75]. It may thus be important to test multiple 3D models. Some cells form loose aggregates at best rather than true spheroids, hence lack the biological properties of a 3D structure and incur difficulties with transfer or manipulations[76]. Furthermore, cell line-derived multicellular spheroids lack cell heterogeneity and immune cell interaction which are known to influence tumor cell response. One way to overcome this is to use a panel of cell lines to better represent patient tumor heterogeneity (genetic and epigenetic variations)[80 143], as was done in this study. Furthermore, it is important to consider in what setting (chemotherapy-naïve, recurrence, etc.) the cell lines were derived to correspond to the study objectives. Culture techniques may also play a role in cell phenotype and viability. Using human bone marrow mesenchymal stem cells, Deng et al reported a difference in cell morphology (more round in non-adherent culture) and viability (higher apoptosis rate after 72 hours when cells cultured in ULA plates compared to standard adherent tissue culture plates)[144]. Although this was not studied with cancer cells, this may in part effect the baseline cell viability and chemoresponse when using different models. Newer cancer models are designed to improve some of these shortcomings.

Currently there are few adequate 3D analysis methods that allows us to maintain the biological structure intact and often researchers rely on 2D methods[70 80 130]. These manipulations can induce phenotypic changes and decrease viability[96]. Immunohistochemistry is often used with tissues, however in spheroids, deformation and fracture are not uncommon from cutting, and poor contrast of stains, low spatial resolution and inability to capture dynamic events make this analysis method less attractive[145]. However, there is growing knowledge on the use of tools such as confocal microscopy to enable the analysis of 3D models[95 130 146]. The latter allows to appreciate the overall shape of the 3D model as well as the localization of cells[95 107 146], however visualization of the inner layer of cells of spheroids over 100μm can be challenging due to poor light penetration[70] and may have photo-toxic effects for long-term imaging[147]. Traditional fluorescence microscopy for 3D models such as spheroids make observations in high resolution, in depth and in real time challenging[147]. Evaluation of drug diffusion in the core of a 3D model for example would be impossible with confocal microscopy but with a newer technology called light sheet microscopy (LSM), submicron imaging of molecule diffusion can be visualized[148]. LSM also offers ultra-low intensity of light excitation (200x less energy than confocal[145]) so minimal photo-toxic effects are expected. In addition, tissue clearing is a method that can render tissue samples (human, rodents) optically clear and retain its 3D structure to remove any inner eclipsing effects while allowing staining[147]. The latter allows appreciation of expression across the entire tissue. LSM can also be used with microdevices such as with ex-vivo models in microfluidics devices[147]. Furthermore, given the variable penetration of agents, one must consider the possibility that dyes used for viability testing may not penetrate the spheroid uniformly and thus under-represent the parameter being evaluated[70 106].

The challenges with traditional in vivo models

Animal models, especially murine models, are often considered the gold standard *in vivo* preclinical model prior to clinical trial design. However, there are still important differences with humans that can account for some of the discrepancies seen in drug efficacy, including "basal metabolic rate, cytogenic profile, fibroblast immortalization and tumor-suppressor pathways"[98]. Using appropriate endpoints is also important in preclinical model use. For intervention therapy studies, including the OS increases the predictive power of a preclinical study[65 149]. Furthermore, statistically significant response in a single model does not equate to clinically relevant response. In fact the National Cancer Institute (NCI) and the Canadian Cancer Trials Group (CCTG) have found that drug prediction increases when more than one model is used and xenograft growth inhibition exceeds 60% for clinical effect[66].

Perspectives

The results in this study shed light on some of the challenges with preclinical model development and therapeutic response. It has implications in regard to future studies that could be carried out to solve unanswered questions and also has implications for the ovarian cancer community at large.

As previously mentioned, hypoxia appears to play a key in drug response in 3D spheroids. In our studies, the two cell lines for which spheroid response did not correlate with that seen *in vivo* (OV4453 and OV4485) were cultured in conditions of low oxygen because they grow slower in lower oxygen. Therefore, albeit this difficulty, it will be important to test the carboplatin response of spheroids of these two cell lines in normal oxygen conditions to better compare response with the other cell lines. Furthermore, we are currently evaluating the carboplatin response of the same

6 cell lines used in this work in a 3D *ex-vivo* micro-dissected tumor model[138]. Briefly, this model consists of dissecting tumor into fragments of 400µm and inserting them into microfluidics chips where they are cultured and treated. To analyse response to treatment, micro-dissected tumor microarrays are created and viability assays using immunofluorescence are performed. Xenografts from the control-treated mice from our study are used as tissue material and inserted into the microwells of the microfluidic device. We await the results of these studies to correlate them with *in vivo* responses.

Another aspect that could be further explored in a future study is to better understand the impact of MDR gene expression differences across different model systems and how it affects drug response. This can be performed through a molecular approach with RNA sequencing or microarray analysis in all three models to study the differences in carboplatin response in the EOC cell lines. Furthermore, although carboplatin is currently most clinically relevant for EOC patients, it would be interesting to perform a similar study with other drugs, such as paclitaxel, bevacizumab and PARPis.

EOC is a complex and heterogenous disease. For now, platinum therapy is still an integral part of treatment for patients, however chemoresistance remains an important obstacle with dismal survival and limited options at this stage of disease progression. With the significant investment of 10 million dollars that the Canadian government has afforded to ovarian cancer research, one of the top three priorities remains the development of better experimental models. With the overall high attrition rate of oncologic treatments, it is crucial to invest upfront in more cost-effective predictive cancer models. This study highlights the heterogenous therapeutic response seen with cancer cell lines when culture in different model systems and speaks to using the right model for drug screening and prediction studies.

The use of sophisticated experimental models becomes even more relevant for drug discovery and testing in rare cancers[61]. As clinical trials are challenging in these cases, relying on better preclinical models to guide and screen novel and combination drugs becomes more important. Furthermore, this could help reduce the rate of failed clinical trials as well as avoid unnecessary toxicities and treatment delays in patients that are unresponsive to a 'standard' treatment. In fact, in the era of personalized medicine, it would be ideal to optimize treatment selection based on individual tumor and patient characteristics, rather than a 'one treatment for all' approach.

Chapter 5 – Conclusion

In conclusion, it is important that the research community involved in drug discovery and/or drug screening consider many factors when selecting a preclinical model. Although cell line-based models have received criticisms, it remains an important, reproducible and inexpensive model. However, a better understanding of biological differences that dictates drug response *in vitro* and *in vivo* are essential in order to improve the success rate of the drug discovery pipeline. This may avoid rejecting potentially effective drugs as well as eliminating ineffective drugs from clinical trials. Validation and feasibility studies of newer more complex *in vitro* and *in vivo* models are still needed to enhance the current standards.

References

1. Committee CCSA. Canadian Cancer

Statistics 2019. In: Society CC, ed. Toronto, Ontario: Canadian Cancer Society, 2019.

2. Siegel RL, Miller KD, Jemal A. Cancer statistics, 2019. *CA Cancer J Clin* 2019;69(1):7-34. doi: 10.3322/caac.21551 [published Online First: 2019/01/08]
3. Howlader N, Noone A, Krapcho M, et al. SEER Cancer Statistics Review, 1975-2017, National Cancer Institute. Bethesda, MD: National Cancer Institute; 2020 [based on November 2019 SEER data submission, posted to the SEER web site]. Available from: https://seer.cancer.gov/csr/1975_2017/.
4. Al Habyan S, Kalos C, Szymborski J, et al. Multicellular detachment generates metastatic spheroids during intra-abdominal dissemination in epithelial ovarian cancer. *Oncogene* 2018;37(37):5127-35. doi: 10.1038/s41388-018-0317-x [published Online First: 2018/05/23]
5. Konstantinopoulos PA, Matulonis UA. Current status and evolution of preclinical drug development models of epithelial ovarian cancer. *Front Oncol* 2013;3:296. doi: 10.3389/fonc.2013.00296 [published Online First: 2013/12/11]
6. Lheureux S, Gourley C, Vergote I, et al. Epithelial ovarian cancer. *Lancet* 2019;393(10177):1240-53. doi: 10.1016/S0140-6736(18)32552-2
7. Wojnarowicz PM, Oros KK, Quinn MC, et al. The genomic landscape of TP53 and p53 annotated high grade ovarian serous carcinomas from a defined founder population associated with patient outcome. *PLoS One* 2012;7(9):e45484. doi: 10.1371/journal.pone.0045484 [published Online First: 2012/09/20]
8. Ahmed AA, Etemadmoghadam D, Temple J, et al. Driver mutations in TP53 are ubiquitous in high grade serous carcinoma of the ovary. *J Pathol* 2010;221(1):49-56. doi: 10.1002/path.2696
9. Network CGAR. Integrated genomic analyses of ovarian carcinoma. *Nature* 2011;474(7353):609-15. doi: 10.1038/nature10166 [published Online First: 2011/06/29]
10. McAlpine JN, Porter H, Köbel M, et al. BRCA1 and BRCA2 mutations correlate with TP53 abnormalities and presence of immune cell infiltrates in ovarian high-grade serous carcinoma. *Mod Pathol* 2012;25(5):740-50. doi: 10.1038/modpathol.2011.211 [published Online First: 2012/01/27]
11. Bashashati A, Ha G, Tone A, et al. Distinct evolutionary trajectories of primary high-grade serous ovarian cancers revealed through spatial mutational profiling. *J Pathol* 2013;231(1):21-34. doi: 10.1002/path.4230
12. Alkema NG, Wisman GB, van der Zee AG, et al. Studying platinum sensitivity and resistance in high-grade serous ovarian cancer: Different models for different questions. *Drug Resist Updat* 2016;24:55-69. doi: 10.1016/j.drup.2015.11.005 [published Online First: 2015/11/26]
13. Lord CJ, Ashworth A. BRCAness revisited. *Nat Rev Cancer* 2016;16(2):110-20. doi: 10.1038/nrc.2015.21 [published Online First: 2016/01/18]

14. Daly MB, Pilarski R, Yurgelun MB, et al. NCCN Guidelines Insights: Genetic/Familial High-Risk Assessment: Breast, Ovarian, and Pancreatic, Version 1.2020. *J Natl Compr Canc Netw* 2020;18(4):380-91. doi: 10.6004/jnccn.2020.0017 [published Online First: 2020/04/08]
15. Konstantinopoulos PA, Norquist B, Lacchetti C, et al. Germline and Somatic Tumor Testing in Epithelial Ovarian Cancer: ASCO Guideline. *J Clin Oncol* 2020;38(11):1222-45. doi: 10.1200/JCO.19.02960 [published Online First: 2020/01/27]
16. Gupta S, Provenzale D, Llor X, et al. NCCN Guidelines Insights: Genetic/Familial High-Risk Assessment: Colorectal, Version 2.2019. *J Natl Compr Canc Netw* 2019;17(9):1032-41. doi: 10.6004/jnccn.2019.0044 [published Online First: 2019/09/06]
17. Marcus L, Lemery SJ, Keegan P, et al. FDA Approval Summary: Pembrolizumab for the Treatment of Microsatellite Instability-High Solid Tumors. *Clin Cancer Res* 2019;25(13):3753-58. doi: 10.1158/1078-0432.ccr-18-4070 [published Online First: 2019/02/23]
18. Boyiadzis MM, Kirkwood JM, Marshall JL, et al. Significance and implications of FDA approval of pembrolizumab for biomarker-defined disease. *J Immunother Cancer* 2018;6(1):35. doi: 10.1186/s40425-018-0342-x [published Online First: 2018/05/15]
19. Vergote I, Tropé CG, Amant F, et al. Neoadjuvant chemotherapy or primary surgery in stage IIIC or IV ovarian cancer. *N Engl J Med* 2010;363(10):943-53. doi: 10.1056/NEJMoa0908806
20. Kehoe S, Hook J, Nankivell M, et al. Primary chemotherapy versus primary surgery for newly diagnosed advanced ovarian cancer (CHORUS): an open-label, randomised, controlled, non-inferiority trial. *Lancet* 2015;386(9990):249-57. doi: 10.1016/S0140-6736(14)62223-6 [published Online First: 2015/05/19]
21. Tangjitgamol S, Manusirivithaya S, Laopaiboon M, et al. Interval debulking surgery for advanced epithelial ovarian cancer. *Cochrane Database Syst Rev* 2013(4):CD006014. doi: 10.1002/14651858.CD006014.pub6 [published Online First: 2013/04/30]
22. Tewari D, Java JJ, Salani R, et al. Long-term survival advantage and prognostic factors associated with intraperitoneal chemotherapy treatment in advanced ovarian cancer: a gynecologic oncology group study. *J Clin Oncol* 2015;33(13):1460-6. doi: 10.1200/JCO.2014.55.9898 [published Online First: 2015/03/23]
23. van Driel WJ, Koole SN, Sikorska K, et al. Hyperthermic Intraperitoneal Chemotherapy in Ovarian Cancer. *N Engl J Med* 2018;378(3):230-40. doi: 10.1056/NEJMoa1708618
24. Burger RA, Brady MF, Bookman MA, et al. Incorporation of bevacizumab in the primary treatment of ovarian cancer. *N Engl J Med* 2011;365(26):2473-83. doi: 10.1056/NEJMoa1104390
25. Oza AM, Cook AD, Pfisterer J, et al. Standard chemotherapy with or without bevacizumab for women with newly diagnosed ovarian cancer (ICON7): overall survival results of a phase 3 randomised trial. *Lancet Oncol* 2015;16(8):928-36. doi: 10.1016/S1470-2045(15)00086-8 [published Online First: 2015/06/23]
26. Marabelle A, Le DT, Ascierto PA, et al. Efficacy of Pembrolizumab in Patients With Noncolorectal High Microsatellite Instability/Mismatch Repair-Deficient Cancer: Results From the Phase II KEYNOTE-158 Study. *J Clin Oncol* 2020;38(1):1-10. doi: 10.1200/jco.19.02105 [published Online First: 2019/11/05]

27. González-Martín A, Pothuri B, Vergote I, et al. Niraparib in Patients with Newly Diagnosed Advanced Ovarian Cancer. *N Engl J Med* 2019;381(25):2391-402. doi: 10.1056/NEJMoa1910962 [published Online First: 2019/09/29]
28. Moore K, Colombo N, Scambia G, et al. Maintenance Olaparib in Patients with Newly Diagnosed Advanced Ovarian Cancer. *N Engl J Med* 2018;379(26):2495-505. doi: 10.1056/NEJMoa1810858 [published Online First: 2018/10/23]
29. Gershenson DM, Bodurka DC, Coleman RL, et al. Hormonal Maintenance Therapy for Women With Low-Grade Serous Cancer of the Ovary or Peritoneum. *J Clin Oncol* 2017;35(10):1103-11. doi: 10.1200/JCO.2016.71.0632 [published Online First: 2017/02/21]
30. Wilson MK, Pujade-Lauraine E, Aoki D, et al. Fifth Ovarian Cancer Consensus Conference of the Gynecologic Cancer InterGroup: recurrent disease. *Ann Oncol* 2017;28(4):727-32. doi: 10.1093/annonc/mdw663
31. Ricciardelli C, Lokman NA, Sabit I, et al. Novel ex vivo ovarian cancer tissue explant assay for prediction of chemosensitivity and response to novel therapeutics. *Cancer Lett* 2018;421:51-58. doi: 10.1016/j.canlet.2018.02.006 [published Online First: 2018/02/06]
32. Harter P, du Bois A, Hahmann M, et al. Surgery in recurrent ovarian cancer: the Arbeitsgemeinschaft Gynaekologische Onkologie (AGO) DESKTOP OVAR trial. *Ann Surg Oncol* 2006;13(12):1702-10. doi: 10.1245/s10434-006-9058-0
33. Burger RA, Sill MW, Monk BJ, et al. Phase II trial of bevacizumab in persistent or recurrent epithelial ovarian cancer or primary peritoneal cancer: a Gynecologic Oncology Group Study. *J Clin Oncol* 2007;25(33):5165-71. doi: 10.1200/JCO.2007.11.5345
34. Aghajanian C, Blank SV, Goff BA, et al. OCEANS: a randomized, double-blind, placebo-controlled phase III trial of chemotherapy with or without bevacizumab in patients with platinum-sensitive recurrent epithelial ovarian, primary peritoneal, or fallopian tube cancer. *J Clin Oncol* 2012;30(17):2039-45. doi: 10.1200/JCO.2012.42.0505 [published Online First: 2012/04/23]
35. Coleman RL, Brady MF, Herzog TJ, et al. Bevacizumab and paclitaxel-carboplatin chemotherapy and secondary cytoreduction in recurrent, platinum-sensitive ovarian cancer (NRG Oncology/Gynecologic Oncology Group study GOG-0213): a multicentre, open-label, randomised, phase 3 trial. *Lancet Oncol* 2017;18(6):779-91. doi: 10.1016/S1470-2045(17)30279-6 [published Online First: 2017/04/21]
36. Pujade-Lauraine E, Hilpert F, Weber B, et al. Bevacizumab combined with chemotherapy for platinum-resistant recurrent ovarian cancer: The AURELIA open-label randomized phase III trial. *J Clin Oncol* 2014;32(13):1302-8. doi: 10.1200/JCO.2013.51.4489 [published Online First: 2014/03/17]
37. Mirza MR, Åvall Lundqvist E, Birrer MJ, et al. Niraparib plus bevacizumab versus niraparib alone for platinum-sensitive recurrent ovarian cancer (NSGO-AVANOVA2/ENGOT-ov24): a randomised, phase 2, superiority trial. *Lancet Oncol* 2019;20(10):1409-19. doi: 10.1016/S1470-2045(19)30515-7 [published Online First: 2019/08/29]
38. Pujade-Lauraine E, Ledermann JA, Selle F, et al. Olaparib tablets as maintenance therapy in patients with platinum-sensitive, relapsed ovarian cancer and a BRCA1/2 mutation (SOLO2/ENGOT-Ov21): a double-blind, randomised, placebo-controlled, phase 3 trial.

Lancet Oncol 2017;18(9):1274-84. doi: 10.1016/S1470-2045(17)30469-2 [published Online First: 2017/07/25]
39. Mirza MR, Monk BJ, Herrstedt J, et al. Niraparib Maintenance Therapy in Platinum-Sensitive, Recurrent Ovarian Cancer. *N Engl J Med* 2016;375(22):2154-64. doi: 10.1056/NEJMoa1611310 [published Online First: 2016/10/07]
40. Le Page C, Huntsman DG, Provencher DM, et al. Predictive and prognostic protein biomarkers in epithelial ovarian cancer: recommendation for future studies. *Cancers (Basel)* 2010;2(2):913-54. doi: 10.3390/cancers2020913 [published Online First: 2010/05/26]
41. Le Page C, Chung J, Rahimi K, et al. Exploring the Clinical Impact of Predictive Biomarkers in Serous Ovarian Carcinomas. *Curr Drug Targets* 2019 doi: 10.2174/1389450120666191016143836 [published Online First: 2019/10/16]
42. Henderson JT, Webber EM, Sawaya GF. Screening for Ovarian Cancer: Updated Evidence Report and Systematic Review for the US Preventive Services Task Force. *JAMA* 2018;319(6):595-606. doi: 10.1001/jama.2017.21421
43. Rustin GJ, van der Burg ME, Griffin CL, et al. Early versus delayed treatment of relapsed ovarian cancer (MRC OV05/EORTC 55955): a randomised trial. *Lancet* 2010;376(9747):1155-63. doi: 10.1016/S0140-6736(10)61268-8
44. Pignata S, Cannella L, Leopardo D, et al. Follow-up with CA125 after primary therapy of advanced ovarian cancer: in favor of continuing to prescribe CA125 during follow-up. *Ann Oncol* 2011;22 Suppl 8:viii40-viii44. doi: 10.1093/annonc/mdr470
45. Whitwell HJ, Worthington J, Blyuss O, et al. Improved early detection of ovarian cancer using longitudinal multimarker models. *Br J Cancer* 2020;122(6):847-56. doi: 10.1038/s41416-019-0718-9 [published Online First: 2020/01/15]
46. Poveda A, Floquet A, Ledermann JA, et al. Final overall survival (OS) results from SOLO2/ENGOT-ov21: A phase III trial assessing maintenance olaparib in patients (pts) with platinum-sensitive, relapsed ovarian cancer and a BRCA mutation. *Journal of Clinical Oncology* 2020;38(15_suppl):6002-02. doi: 10.1200/JCO.2020.38.15_suppl.6002
47. Rivera D, Paudice M, Gismondi V, et al. Implementing NGS-based. *J Clin Pathol* 2020 doi: 10.1136/jclinpath-2020-206840 [published Online First: 2020/09/07]
48. Miller RE, Leary A, Scott CL, et al. ESMO recommendations on predictive biomarker testing for homologous recombination deficiency and PARP inhibitor benefit in ovarian cancer. *Ann Oncol* 2020 doi: 10.1016/j.annonc.2020.08.2102 [published Online First: 2020/09/28]
49. Stover EH, Fuh K, Konstantinopoulos PA, et al. Clinical assays for assessment of homologous recombination DNA repair deficiency. *Gynecol Oncol* 2020 doi: 10.1016/j.ygyno.2020.09.029 [published Online First: 2020/10/01]
50. Llaurado Fernandez M, Dawson A, Kim H, et al. Hormone receptor expression and outcomes in low-grade serous ovarian carcinoma. *Gynecol Oncol* 2020;157(1):12-20. doi: 10.1016/j.ygyno.2019.11.029 [published Online First: 2020/01/20]
51. Fader AN. A Randomized Phase III, Two-Arm Trial of Paclitaxel/Carboplatin/Maintenance Letrozole Versus Letrozole Monotherapy in Patients With Stage II-IV, Primary Low-Grade Serous Carcinoma of the Ovary or Peritoneum [Available from: https://clinicaltrials.gov/ct2/show/NCT04095364.

52. Alldredge J, Serna-Gallegos T, Gallegos N, et al. Evaluation of clear cell subtypes of ovarian and uterine malignancies with anti-PD-L1 and anti-PD1 immunohistochemical expression and their association with stage and survival. *Gynecol Oncol* 2019;155(3):483-88. doi: 10.1016/j.ygyno.2019.10.008 [published Online First: 2019/10/28]
53. Hamanishi J, Mandai M, Ikeda T, et al. Safety and Antitumor Activity of Anti-PD-1 Antibody, Nivolumab, in Patients With Platinum-Resistant Ovarian Cancer. *J Clin Oncol* 2015;33(34):4015-22. doi: 10.1200/JCO.2015.62.3397 [published Online First: 2015/09/08]
54. Matulonis UA, Shapira-Frommer R, Santin AD, et al. Antitumor activity and safety of pembrolizumab in patients with advanced recurrent ovarian cancer: results from the phase II KEYNOTE-100 study. *Ann Oncol* 2019;30(7):1080-87. doi: 10.1093/annonc/mdz135
55. Moore KN, Secord AA, Geller MA, et al. Niraparib monotherapy for late-line treatment of ovarian cancer (QUADRA): a multicentre, open-label, single-arm, phase 2 trial. *Lancet Oncol* 2019;20(5):636-48. doi: 10.1016/S1470-2045(19)30029-4 [published Online First: 2019/04/01]
56. Sandhu SK, Schelman WR, Wilding G, et al. The poly(ADP-ribose) polymerase inhibitor niraparib (MK4827) in BRCA mutation carriers and patients with sporadic cancer: a phase 1 dose-escalation trial. *Lancet Oncol* 2013;14(9):882-92. doi: 10.1016/S1470-2045(13)70240-7 [published Online First: 2013/06/28]
57. Lovitt CJ, Shelper TB, Avery VM. Cancer drug discovery: recent innovative approaches to tumor modeling. *Expert Opin Drug Discov* 2016;11(9):885-94. doi: 10.1080/17460441.2016.1214562
58. Cunnea P, Stronach EA. Modeling platinum sensitive and resistant high-grade serous ovarian cancer: development and applications of experimental systems. *Front Oncol* 2014;4:81. doi: 10.3389/fonc.2014.00081 [published Online First: 2014/04/17]
59. Gao H, Korn JM, Ferretti S, et al. High-throughput screening using patient-derived tumor xenografts to predict clinical trial drug response. *Nat Med* 2015;21(11):1318-25. doi: 10.1038/nm.3954 [published Online First: 2015/10/19]
60. Aihara A, Abe N, Saruhashi K, et al. Novel 3-D cell culture system for in vitro evaluation of anticancer drugs under anchorage-independent conditions. *Cancer Sci* 2016;107(12):1858-66. doi: 10.1111/cas.13095 [published Online First: 2016/12/19]
61. Colella G, Fazioli F, Gallo M, et al. Sarcoma Spheroids and Organoids-Promising Tools in the Era of Personalized Medicine. *Int J Mol Sci* 2018;19(2) doi: 10.3390/ijms19020615 [published Online First: 2018/02/21]
62. Boone JD, Dobbin ZC, Straughn JM, et al. Ovarian and cervical cancer patient derived xenografts: The past, present, and future. *Gynecol Oncol* 2015;138(2):486-91. doi: 10.1016/j.ygyno.2015.05.022 [published Online First: 2015/05/27]
63. Tudrej P, Kujawa KA, Cortez AJ, et al. Characteristics of in Vivo Model Systems for Ovarian Cancer Studies. *Diagnostics (Basel)* 2019;9(3) doi: 10.3390/diagnostics9030120 [published Online First: 2019/09/14]
64. Magnotti E, Marasco WA. The latest animal models of ovarian cancer for novel drug discovery. *Expert Opin Drug Discov* 2018;13(3):249-57. doi: 10.1080/17460441.2018.1426567 [published Online First: 2018/01/17]

65. Day CP, Merlino G, Van Dyke T. Preclinical mouse cancer models: a maze of opportunities and challenges. *Cell* 2015;163(1):39-53. doi: 10.1016/j.cell.2015.08.068
66. Gould SE, Junttila MR, de Sauvage FJ. Translational value of mouse models in oncology drug development. *Nat Med* 2015;21(5):431-9. doi: 10.1038/nm.3853
67. Bregenzer ME, Davis C, Horst EN, et al. Physiologic Patient Derived 3D Spheroids for Anti-neoplastic Drug Screening to Target Cancer Stem Cells. *J Vis Exp* 2019(149) doi: 10.3791/59696 [published Online First: 2019/07/05]
68. Erlichman C, Vidgen D. Cytotoxicity of adriamycin in MGH-U1 cells grown as monolayer cultures, spheroids, and xenografts in immune-deprived mice. *Cancer Res* 1984;44(11):5369-75.
69. Chatzinikolaidou M. Cell spheroids: the new frontiers in in vitro models for cancer drug validation. *Drug Discov Today* 2016;21(9):1553-60. doi: 10.1016/j.drudis.2016.06.024 [published Online First: 2016/06/29]
70. Zanoni M, Pignatta S, Arienti C, et al. Anticancer drug discovery using multicellular tumor spheroid models. *Expert Opin Drug Discov* 2019;14(3):289-301. doi: 10.1080/17460441.2019.1570129 [published Online First: 2019/01/28]
71. Hamilton G, Rath B. Applicability of tumor spheroids for. *Expert Opin Drug Metab Toxicol* 2019;15(1):15-23. doi: 10.1080/17425255.2019.1554055 [published Online First: 2018/12/02]
72. Turetta M, Ben FD, Brisotto G, et al. Emerging Technologies for Cancer Research: Towards Personalized Medicine with Microfluidic Platforms and 3D Tumor Models. *Curr Med Chem* 2018;25(35):4616-37. doi: 10.2174/0929867325666180605122633
73. Katt ME, Placone AL, Wong AD, et al. In Vitro Tumor Models: Advantages, Disadvantages, Variables, and Selecting the Right Platform. *Front Bioeng Biotechnol* 2016;4:12. doi: 10.3389/fbioe.2016.00012 [published Online First: 2016/02/12]
74. Sarisozen C, Abouzeid AH, Torchilin VP. The effect of co-delivery of paclitaxel and curcumin by transferrin-targeted PEG-PE-based mixed micelles on resistant ovarian cancer in 3-D spheroids and in vivo tumors. *Eur J Pharm Biopharm* 2014;88(2):539-50. doi: 10.1016/j.ejpb.2014.07.001 [published Online First: 2014/07/10]
75. Gencoglu MF, Barney LE, Hall CL, et al. Comparative Study of Multicellular Tumor Spheroid Formation Methods and Implications for Drug Screening. *ACS Biomater Sci Eng* 2018;4(2):410-20. doi: 10.1021/acsbiomaterials.7b00069 [published Online First: 2017/03/13]
76. Weiswald LB, Bellet D, Dangles-Marie V. Spherical cancer models in tumor biology. *Neoplasia* 2015;17(1):1-15. doi: 10.1016/j.neo.2014.12.004
77. Stock K, Estrada MF, Vidic S, et al. Capturing tumor complexity in vitro: Comparative analysis of 2D and 3D tumor models for drug discovery. *Sci Rep* 2016;6:28951. doi: 10.1038/srep28951 [published Online First: 2016/07/01]
78. Rodrigues T, Kundu B, Silva-Correia J, et al. Emerging tumor spheroids technologies for 3D in vitro cancer modeling. *Pharmacol Ther* 2018;184:201-11. doi: 10.1016/j.pharmthera.2017.10.018 [published Online First: 2017/10/31]
79. Gong X, Lin C, Cheng J, et al. Generation of Multicellular Tumor Spheroids with Microwell-Based Agarose Scaffolds for Drug Testing. *PLoS One* 2015;10(6):e0130348. doi: 10.1371/journal.pone.0130348 [published Online First: 2015/06/19]

80. Acland M, Mittal P, Lokman NA, et al. Mass Spectrometry Analyses of Multicellular Tumor Spheroids. *Proteomics Clin Appl* 2018;12(3):e1700124. doi: 10.1002/prca.201700124 [published Online First: 2018/02/09]
81. Vinci M, Gowan S, Boxall F, et al. Advances in establishment and analysis of three-dimensional tumor spheroid-based functional assays for target validation and drug evaluation. *BMC Biol* 2012;10:29. doi: 10.1186/1741-7007-10-29 [published Online First: 2012/03/22]
82. Eetezadi S, Evans JC, Shen YT, et al. Ratio-Dependent Synergism of a Doxorubicin and Olaparib Combination in 2D and Spheroid Models of Ovarian Cancer. *Mol Pharm* 2018;15(2):472-85. doi: 10.1021/acs.molpharmaceut.7b00843 [published Online First: 2018/01/22]
83. Patra B, Lateef M, Brodeur M, et al. Carboplatin sensitivity in epithelial ovarian cancer cell lines: The impact of model systems. *PLoS ONE* in press
84. Paullin T, Powell C, Menzie C, et al. Spheroid growth in ovarian cancer alters transcriptome responses for stress pathways and epigenetic responses. *PLoS One* 2017;12(8):e0182930. doi: 10.1371/journal.pone.0182930 [published Online First: 2017/08/09]
85. Lawrenson K, Benjamin E, Turmaine M, et al. In vitro three-dimensional modelling of human ovarian surface epithelial cells. *Cell Prolif* 2009;42(3):385-93. doi: 10.1111/j.1365-2184.2009.00604.x [published Online First: 2009/04/24]
86. Zietarska M, Maugard CM, Filali-Mouhim A, et al. Molecular description of a 3D in vitro model for the study of epithelial ovarian cancer (EOC). *Mol Carcinog* 2007;46(10):872-85. doi: 10.1002/mc.20315
87. Wan X, Li Z, Ye H, et al. Three-dimensional perfused tumour spheroid model for anti-cancer drug screening. *Biotechnol Lett* 2016;38(8):1389-95. doi: 10.1007/s10529-016-2035-1 [published Online First: 2016/05/11]
88. Lee JM, Mhawech-Fauceglia P, Lee N, et al. A three-dimensional microenvironment alters protein expression and chemosensitivity of epithelial ovarian cancer cells in vitro. *Lab Invest* 2013;93(5):528-42. doi: 10.1038/labinvest.2013.41 [published Online First: 2013/03/04]
89. Rizvi I, Celli JP, Evans CL, et al. Synergistic enhancement of carboplatin efficacy with photodynamic therapy in a three-dimensional model for micrometastatic ovarian cancer. *Cancer Res* 2010;70(22):9319-28. doi: 10.1158/0008-5472.CAN-10-1783 [published Online First: 2010/11/09]
90. Shan F, Close DA, Camarco DP, et al. High-Content Screening Comparison of Cancer Drug Accumulation and Distribution in Two-Dimensional and Three-Dimensional Culture Models of Head and Neck Cancer. *Assay Drug Dev Technol* 2018;16(1):27-50. doi: 10.1089/adt.2017.812 [published Online First: 2017/12/07]
91. St-Georges-Robillard A, Cahuzac M, Péant B, et al. Long-term fluorescence hyperspectral imaging of on-chip treated co-culture tumour spheroids to follow clonal evolution. *Integr Biol (Camb)* 2019;11(4):130-41. doi: 10.1093/intbio/zyz012
92. Tung YC, Hsiao AY, Allen SG, et al. High-throughput 3D spheroid culture and drug testing using a 384 hanging drop array. *Analyst* 2011;136(3):473-8. doi: 10.1039/c0an00609b [published Online First: 2010/10/21]

93. Dubois C, Dufour R, Daumar P, et al. Development and cytotoxic response of two proliferative MDA-MB-231 and non-proliferative SUM1315 three-dimensional cell culture models of triple-negative basal-like breast cancer cell lines. *Oncotarget* 2017;8(56):95316-31. doi: 10.18632/oncotarget.20517 [published Online First: 2017/08/24]
94. Raghavan S, Ward MR, Rowley KR, et al. Formation of stable small cell number three-dimensional ovarian cancer spheroids using hanging drop arrays for preclinical drug sensitivity assays. *Gynecol Oncol* 2015;138(1):181-9. doi: 10.1016/j.ygyno.2015.04.014 [published Online First: 2015/04/22]
95. Das T, Meunier L, Barbe L, et al. Empirical chemosensitivity testing in a spheroid model of ovarian cancer using a microfluidics-based multiplex platform. *Biomicrofluidics* 2013;7(1):11805. doi: 10.1063/1.4774309 [published Online First: 2013/01/10]
96. Skardal A, Shupe T, Atala A. Organoid-on-a-chip and body-on-a-chip systems for drug screening and disease modeling. *Drug Discov Today* 2016;21(9):1399-411. doi: 10.1016/j.drudis.2016.07.003 [published Online First: 2016/07/12]
97. Flick MB, O'Malley D, Rutherford T, et al. Apoptosis-based evaluation of chemosensitivity in ovarian cancer patients. *J Soc Gynecol Investig* 2004;11(4):252-9. doi: 10.1016/j.jsgi.2003.11.003
98. Fisher MF, Rao SS. Three-dimensional culture models to study drug resistance in breast cancer. *Biotechnol Bioeng* 2020;117(7):2262-78. doi: 10.1002/bit.27356 [published Online First: 2020/04/27]
99. Fleury H, Communal L, Carmona E, et al. Novel high-grade serous epithelial ovarian cancer cell lines that reflect the molecular diversity of both the sporadic and hereditary disease. *Genes Cancer* 2015;6(9-10):378-98.
100. Ouellet V, Zietarska M, Portelance L, et al. Characterization of three new serous epithelial ovarian cancer cell lines. *BMC Cancer* 2008;8:152. doi: 10.1186/1471-2407-8-152 [published Online First: 2008/05/28]
101. Provencher DM, Lounis H, Champoux L, et al. Characterization of four novel epithelial ovarian cancer cell lines. *In Vitro Cell Dev Biol Anim* 2000;36(6):357-61. doi: 10.1290/1071-2690(2000)0362.0.CO;2
102. Beaufort CM, Helmijr JC, Piskorz AM, et al. Ovarian cancer cell line panel (OCCP): clinical importance of in vitro morphological subtypes. *PLoS One* 2014;9(9):e103988. doi: 10.1371/journal.pone.0103988 [published Online First: 2014/09/17]
103. Pearson T, Shultz LD, Miller D, et al. Non-obese diabetic-recombination activating gene-1 (NOD-Rag1 null) interleukin (IL)-2 receptor common gamma chain (IL2r gamma null) null mice: a radioresistant model for human lymphohaematopoietic engraftment. *Clin Exp Immunol* 2008;154(2):270-84. doi: 10.1111/j.1365-2249.2008.03753.x [published Online First: 2008/09/08]
104. Mombaerts P, Iacomini J, Johnson RS, et al. RAG-1-deficient mice have no mature B and T lymphocytes. *Cell* 1992;68(5):869-77. doi: 10.1016/0092-8674(92)90030-g
105. Synthesis and activity studies in vitro and in vivo of a new series of malonato-platinum(II) complexes containing sulfide and phosphine ligands. *European Journal of Medicinal Chemistry* 1992;27(6):611 - 14. doi: https://doi.org/10.1016/0223-5234(92)90139-R

106. Sokolova E, Kutova O, Grishina A, et al. Penetration Efficiency of Antitumor Agents in Ovarian Cancer Spheroids: The Case of Recombinant Targeted Toxin DARPin-LoPE and the Chemotherapy Drug, Doxorubicin. *Pharmaceutics* 2019;11(5) doi: 10.3390/pharmaceutics11050219 [published Online First: 2019/05/07]
107. Mulholland T, McAllister M, Patek S, et al. Drug screening of biopsy-derived spheroids using a self-generated microfluidic concentration gradient. *Sci Rep* 2018;8(1):14672. doi: 10.1038/s41598-018-33055-0 [published Online First: 2018/10/02]
108. Astolfi M, Péant B, Lateef MA, et al. Micro-dissected tumor tissues on chip: an ex vivo method for drug testing and personalized therapy. *Lab Chip* 2016;16(2):312-25. doi: 10.1039/c5lc01108f
109. Mo L, Pospichalova V, Huang Z, et al. Ascites Increases Expression/Function of Multidrug Resistance Proteins in Ovarian Cancer Cells. *PLoS One* 2015;10(7):e0131579. doi: 10.1371/journal.pone.0131579 [published Online First: 2015/07/06]
110. Rosso M, Majem B, Devis L, et al. E-cadherin: A determinant molecule associated with ovarian cancer progression, dissemination and aggressiveness. *PLoS One* 2017;12(9):e0184439. doi: 10.1371/journal.pone.0184439 [published Online First: 2017/09/21]
111. Hirst J, Pathak HB, Hyter S, et al. Licofelone Enhances the Efficacy of Paclitaxel in Ovarian Cancer by Reversing Drug Resistance and Tumor Stem-like Properties. *Cancer Res* 2018;78(15):4370-85. doi: 10.1158/0008-5472.CAN-17-3993 [published Online First: 2018/06/11]
112. Muñoz-Galván S, Felipe-Abrio B, García-Carrasco M, et al. New markers for human ovarian cancer that link platinum resistance to the cancer stem cell phenotype and define new therapeutic combinations and diagnostic tools. *J Exp Clin Cancer Res* 2019;38(1):234. doi: 10.1186/s13046-019-1245-5 [published Online First: 2019/06/03]
113. Anglesio MS, Wiegand KC, Melnyk N, et al. Type-specific cell line models for type-specific ovarian cancer research. *PLoS One* 2013;8(9):e72162. doi: 10.1371/journal.pone.0072162 [published Online First: 2013/09/04]
114. Medrano M, Communal L, Brown KR, et al. Interrogation of Functional Cell-Surface Markers Identifies CD151 Dependency in High-Grade Serous Ovarian Cancer. *Cell Rep* 2017;18(10):2343-58. doi: 10.1016/j.celrep.2017.02.028
115. Heredia-Soto V, Redondo A, Berjón A, et al. High-throughput 3-dimensional culture of epithelial ovarian cancer cells as preclinical model of disease. *Oncotarget* 2018;9(31):21893-903. doi: 10.18632/oncotarget.25098 [published Online First: 2018/04/24]
116. Shen YT, Evans JC, Zafarana G, et al. BRCA Status Does Not Predict Synergism of a Carboplatin and Olaparib Combination in High-Grade Serous Ovarian Cancer Cell Lines. *Mol Pharm* 2018;15(7):2742-53. doi: 10.1021/acs.molpharmaceut.8b00246 [published Online First: 2018/06/01]
117. Gonzalo Tapia and Ivan D-P. Molecular Mechanisms of Platinum Resistance in Ovarian Cancer. 2013 doi: 10.5772/55562
118. Gao B, Yang F, Chen W, et al. Multidrug resistance affects the prognosis of primary epithelial ovarian cancer. *Oncol Lett* 2019;18(4):4262-69. doi: 10.3892/ol.2019.10745 [published Online First: 2019/08/14]

119. Fink D, Aebi S, Howell SB. The role of DNA mismatch repair in drug resistance. *Clin Cancer Res* 1998;4(1):1-6.
120. Raghavan S, Mehta P, Ward MR, et al. Personalized Medicine-Based Approach to Model Patterns of Chemoresistance and Tumor Recurrence Using Ovarian Cancer Stem Cell Spheroids. *Clin Cancer Res* 2017;23(22):6934-45. doi: 10.1158/1078-0432.CCR-17-0133 [published Online First: 2017/08/16]
121. Leung M, Kievit FM, Florczyk SJ, et al. Chitosan-alginate scaffold culture system for hepatocellular carcinoma increases malignancy and drug resistance. *Pharm Res* 2010;27(9):1939-48. doi: 10.1007/s11095-010-0198-3 [published Online First: 2010/06/29]
122. Brancato V, Gioiella F, Imparato G, et al. 3D breast cancer microtissue reveals the role of tumor microenvironment on the transport and efficacy of free-doxorubicin in vitro. *Acta Biomater* 2018;75:200-12. doi: 10.1016/j.actbio.2018.05.055 [published Online First: 2018/06/01]
123. Létourneau IJ, Quinn MC, Wang LL, et al. Derivation and characterization of matched cell lines from primary and recurrent serous ovarian cancer. *BMC Cancer* 2012;12:379. doi: 10.1186/1471-2407-12-379 [published Online First: 2012/08/29]
124. Viscarra T, Buchegger K, Jofre I, et al. Functional and transcriptomic characterization of carboplatin-resistant A2780 ovarian cancer cell line. *Biol Res* 2019;52(1):13. doi: 10.1186/s40659-019-0220-0 [published Online First: 2019/03/21]
125. Moreno-Smith M, Halder JB, Meltzer PS, et al. ATP11B mediates platinum resistance in ovarian cancer. *J Clin Invest* 2013;123(5):2119-30. doi: 10.1172/JCI65425 [published Online First: 2013/04/15]
126. Helleman J, Smid M, Jansen MP, et al. Pathway analysis of gene lists associated with platinum-based chemotherapy resistance in ovarian cancer: the big picture. *Gynecol Oncol* 2010;117(2):170-6. doi: 10.1016/j.ygyno.2010.01.010 [published Online First: 2010/02/04]
127. Diaz Osterman CJ, Ozmadenci D, Kleinschmidt EG, et al. FAK activity sustains intrinsic and acquired ovarian cancer resistance to platinum chemotherapy. *Elife* 2019;8 doi: 10.7554/eLife.47327 [published Online First: 2019/09/03]
128. Yang Z, Zhao X. A 3D model of ovarian cancer cell lines on peptide nanofiber scaffold to explore the cell-scaffold interaction and chemotherapeutic resistance of anticancer drugs. *Int J Nanomedicine* 2011;6:303-10. doi: 10.2147/IJN.S15279 [published Online First: 2011/02/02]
129. Mirzayans R, Andrais B, Murray D. Impact of Premature Senescence on Radiosensitivity Measured by High Throughput Cell-Based Assays. *Int J Mol Sci* 2017;18(7) doi: 10.3390/ijms18071460 [published Online First: 2017/07/06]
130. Jabs J, Zickgraf FM, Park J, et al. Screening drug effects in patient-derived cancer cells links organoid responses to genome alterations. *Mol Syst Biol* 2017;13(11):955. doi: 10.15252/msb.20177697 [published Online First: 2017/11/27]
131. Chen H, Gotimer K, De Souza C, et al. Short-term organoid culture for drug sensitivity testing of high-grade serous carcinoma. *Gynecol Oncol* 2020;157(3):783-92. doi: 10.1016/j.ygyno.2020.03.026 [published Online First: 2020/04/04]

132. Kim J, Koo BK, Knoblich JA. Human organoids: model systems for human biology and medicine. *Nat Rev Mol Cell Biol* 2020;21(10):571-84. doi: 10.1038/s41580-020-0259-3 [published Online First: 2020/07/07]
133. Kopper O, de Witte CJ, Lõhmussaar K, et al. An organoid platform for ovarian cancer captures intra- and interpatient heterogeneity. *Nat Med* 2019;25(5):838-49. doi: 10.1038/s41591-019-0422-6 [published Online First: 2019/04/22]
134. Bleijs M, van de Wetering M, Clevers H, et al. Xenograft and organoid model systems in cancer research. *EMBO J* 2019;38(15):e101654. doi: 10.15252/embj.2019101654 [published Online First: 2019/07/08]
135. Weeber F, Ooft SN, Dijkstra KK, et al. Tumor Organoids as a Pre-clinical Cancer Model for Drug Discovery. *Cell Chem Biol* 2017;24(9):1092-100. doi: 10.1016/j.chembiol.2017.06.012 [published Online First: 2017/07/27]
136. Ooft SN, Weeber F, Dijkstra KK, et al. Patient-derived organoids can predict response to chemotherapy in metastatic colorectal cancer patients. *Sci Transl Med* 2019;11(513) doi: 10.1126/scitranslmed.aay2574
137. Masiello T, Dhall A, Hemachandra LPM, et al. A Dynamic Culture Method to Produce Ovarian Cancer Spheroids under Physiologically-Relevant Shear Stress. *Cells* 2018;7(12) doi: 10.3390/cells7120277 [published Online First: 2018/12/19]
138. Simeone K, Guay-Lord R, Lateef MA, et al. Paraffin-embedding lithography and micro-dissected tissue micro-arrays: tools for biological and pharmacological analysis of ex vivo solid tumors. *Lab Chip* 2019;19(4):693-705. doi: 10.1039/c8lc00982a
139. Tian H, Lyu Y, Yang YG, et al. Humanized Rodent Models for Cancer Research. *Front Oncol* 2020;10:1696. doi: 10.3389/fonc.2020.01696 [published Online First: 2020/10/13]
140. Hakozaki T, Richard C, Elkrief A, et al. The Gut Microbiome Associates with Immune Checkpoint Inhibition Outcomes in Patients with Advanced Non-Small Cell Lung Cancer. *Cancer Immunol Res* 2020;8(10):1243-50. doi: 10.1158/2326-6066.CIR-20-0196 [published Online First: 2020/07/27]
141. Gillet JP, Calcagno AM, Varma S, et al. Redefining the relevance of established cancer cell lines to the study of mechanisms of clinical anti-cancer drug resistance. *Proc Natl Acad Sci U S A* 2011;108(46):18708-13. doi: 10.1073/pnas.1111840108 [published Online First: 2011/11/08]
142. Raghavan S, Mehta P, Horst EN, et al. Comparative analysis of tumor spheroid generation techniques for differential in vitro drug toxicity. *Oncotarget* 2016;7(13):16948-61. doi: 10.18632/oncotarget.7659
143. Wilding JL, Bodmer WF. Cancer cell lines for drug discovery and development. *Cancer Res* 2014;74(9):2377-84. doi: 10.1158/0008-5472.CAN-13-2971 [published Online First: 2014/04/09]
144. Deng B, Jiang H, Zeng K, et al. Removal from adherent culture contributes to apoptosis in human bone marrow mesenchymal stem cells. *Mol Med Rep* 2017;15(6):3499-506. doi: 10.3892/mmr.2017.6440 [published Online First: 2017/04/07]
145. Pampaloni F, Ansari N, Stelzer EH. High-resolution deep imaging of live cellular spheroids with light-sheet-based fluorescence microscopy. *Cell Tissue Res* 2013;352(1):161-77. doi: 10.1007/s00441-013-1589-7 [published Online First: 2013/02/27]

146. Eetezadi S, De Souza R, Vythilingam M, et al. Effects of Doxorubicin Delivery Systems and Mild Hyperthermia on Tissue Penetration in 3D Cell Culture Models of Ovarian Cancer Residual Disease. *Mol Pharm* 2015;12(11):3973-85. doi: 10.1021/acs.molpharmaceut.5b00426 [published Online First: 2015/10/02]
147. Andilla J, Jorand R, Olarte OE, et al. Imaging tissue-mimic with light sheet microscopy: A comparative guideline. *Sci Rep* 2017;7:44939. doi: 10.1038/srep44939 [published Online First: 2017/03/21]
148. Lazzari G, Vinciguerra D, Balasso A, et al. Light sheet fluorescence microscopy versus confocal microscopy: in quest of a suitable tool to assess drug and nanomedicine penetration into multicellular tumor spheroids. *Eur J Pharm Biopharm* 2019;142:195-203. doi: 10.1016/j.ejpb.2019.06.019 [published Online First: 2019/06/20]
149. Gengenbacher N, Singhal M, Augustin HG. Preclinical mouse solid tumour models: status quo, challenges and perspectives. *Nat Rev Cancer* 2017;17(12):751-65. doi: 10.1038/nrc.2017.92 [published Online First: 2017/10/27]

Appendix

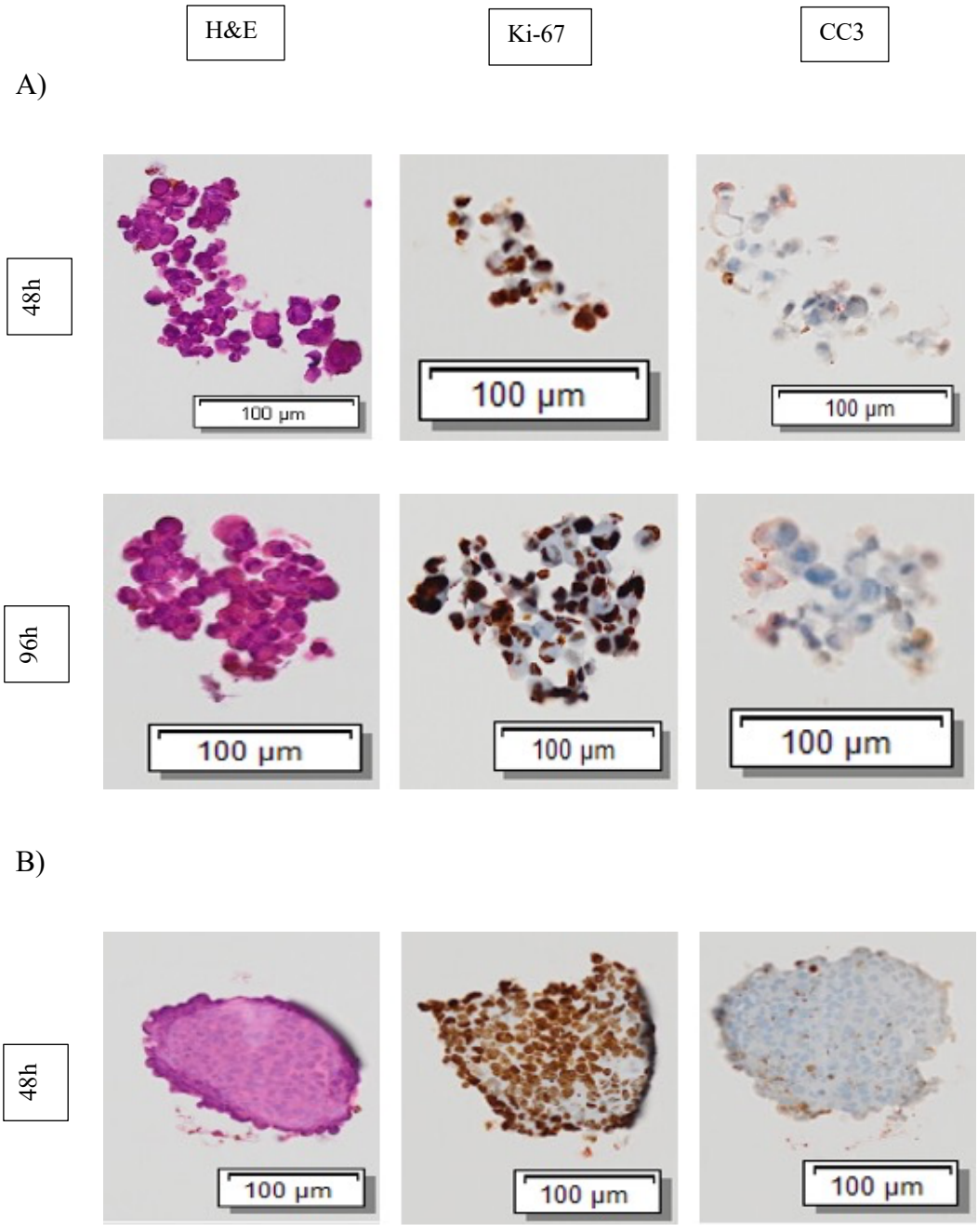

96h

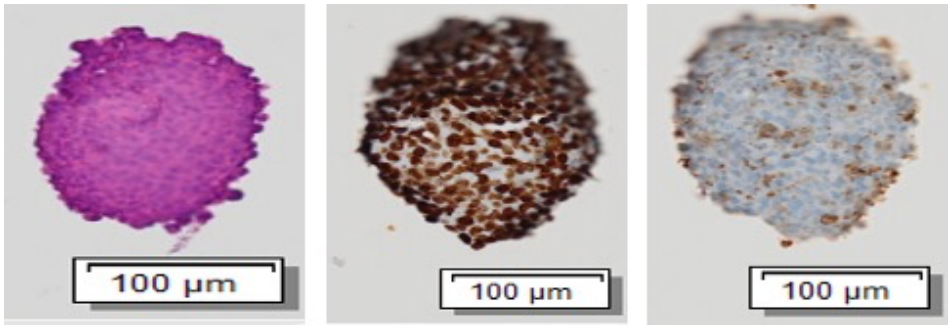

C)

48h

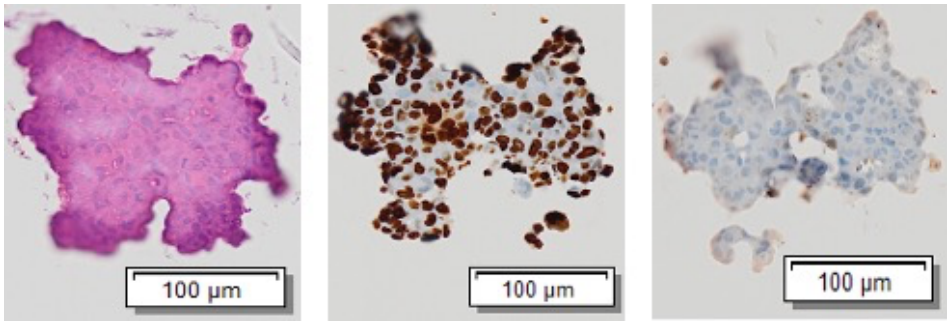

D)

48h

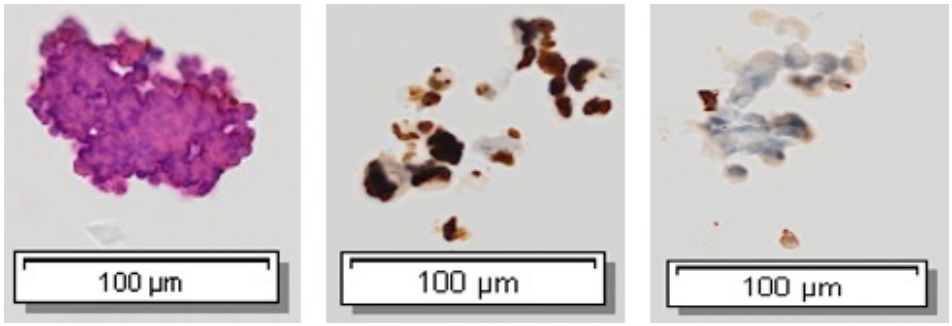

96h

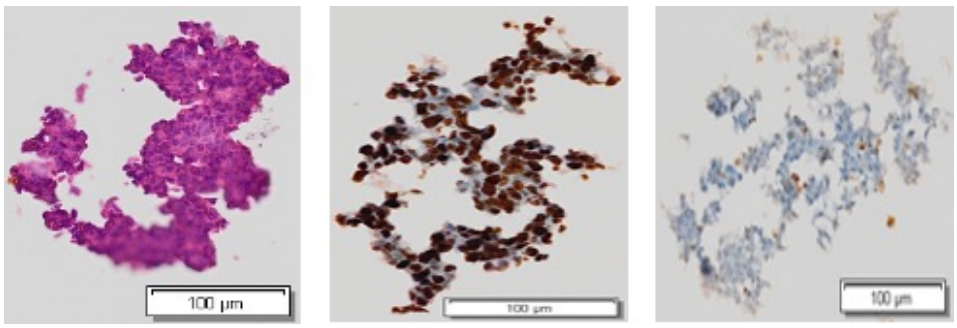

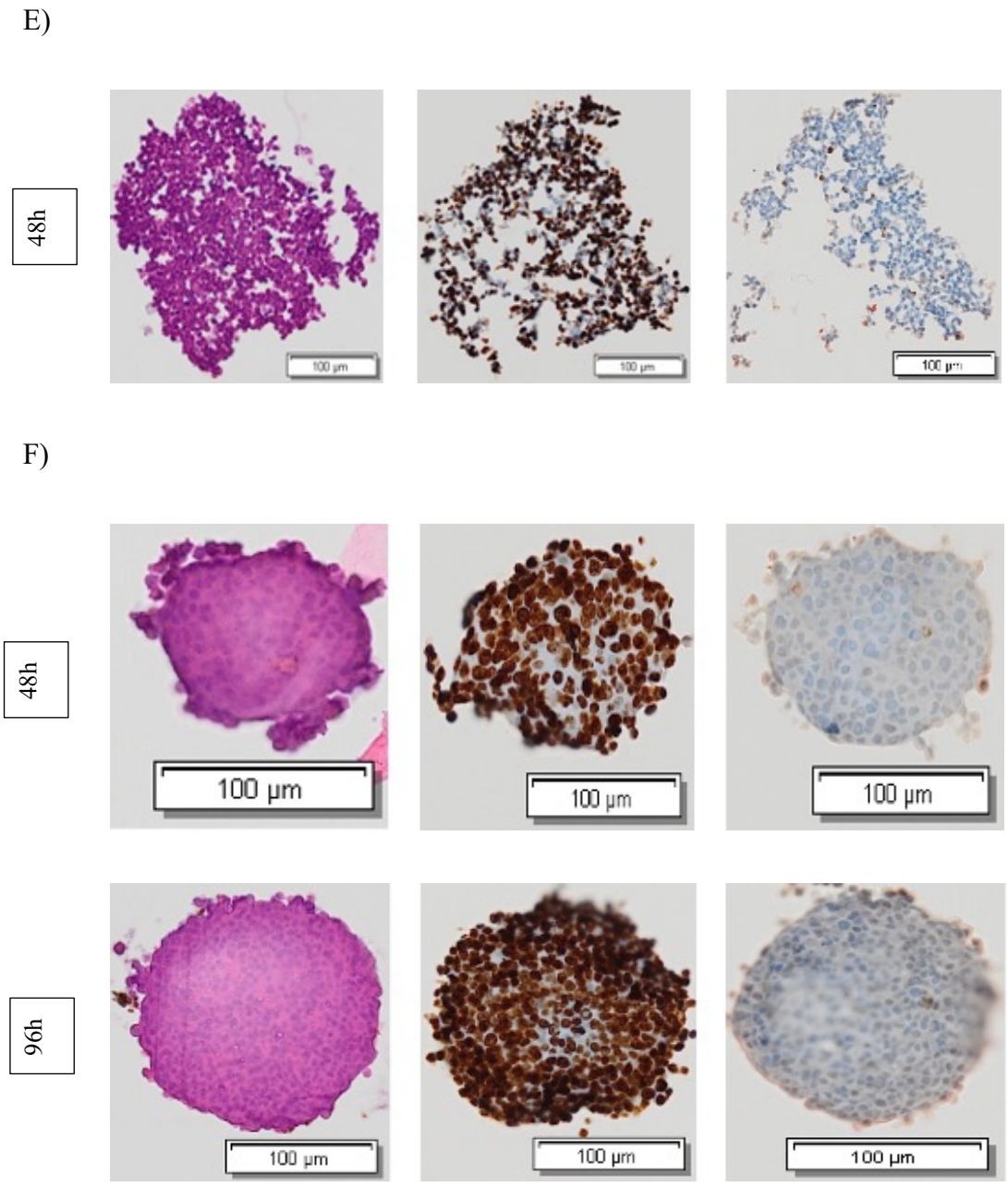

Figure S 1. **Maintenance of spheroid cell viability over a 96-hour period**

A) OV4453 at 48 hours and 96 hours B) OV-1946 at 48 hours and 96 hours C) OV-90 at 48 hours D) OV4485 at 48 hours and 96 hours E) TOV-21G at 48 hours F) TOV-112D at 48 hours and 96 hours. Scale bar = 100µm. Representative photographs were included for stains H&E (left), Ki-67 (middle) and cleaved caspase-3, CC3, (right).

A)

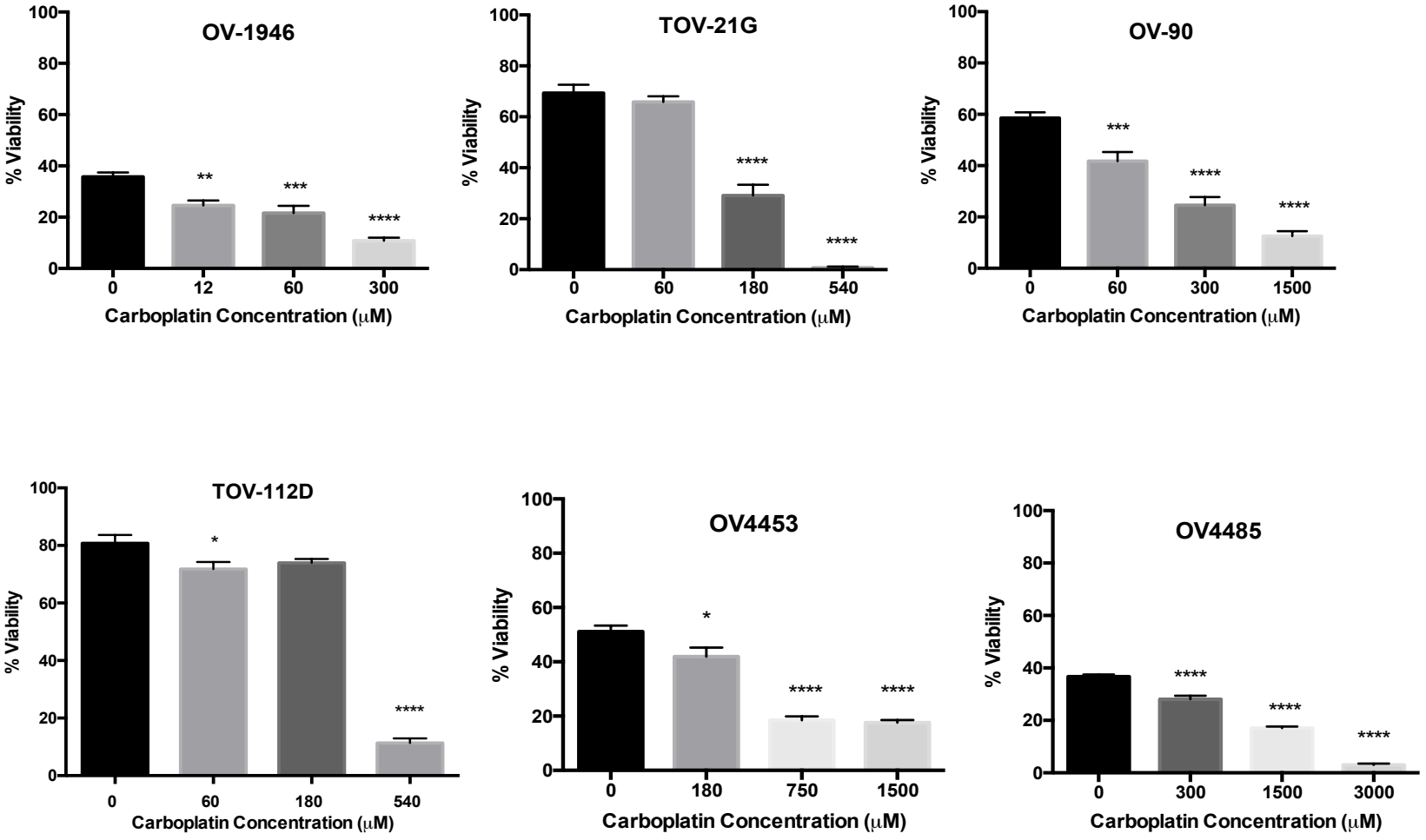
OV-1946
% Viability
100
80
60
40
20
0
**
***
****
0
12
60
300
Carboplatin Concentration (μM)
TOV-21G
% Viability
100
80
60
40
20
0
****
****
0
60
180
540
Carboplatin Concentration (μM)
OV-90
% Viability
100
80
60
40
20
0
***
****
****
0
60
300
1500
Carboplatin Concentration (μM)
TOV-112D
% Viability
100
80
60
40
20
0
*
****
0
60
180
540
Carboplatin Concentration (μM)
OV4453
% Viability
100
80
60
40
20
0
*
****
****
0
180
750
1500
Carboplatin Concentration (μM)
OV4485
% Viability
100
80
60
40
20
0
****
****
****
0
300
1500
3000
Carboplatin Concentration (μM)

B)

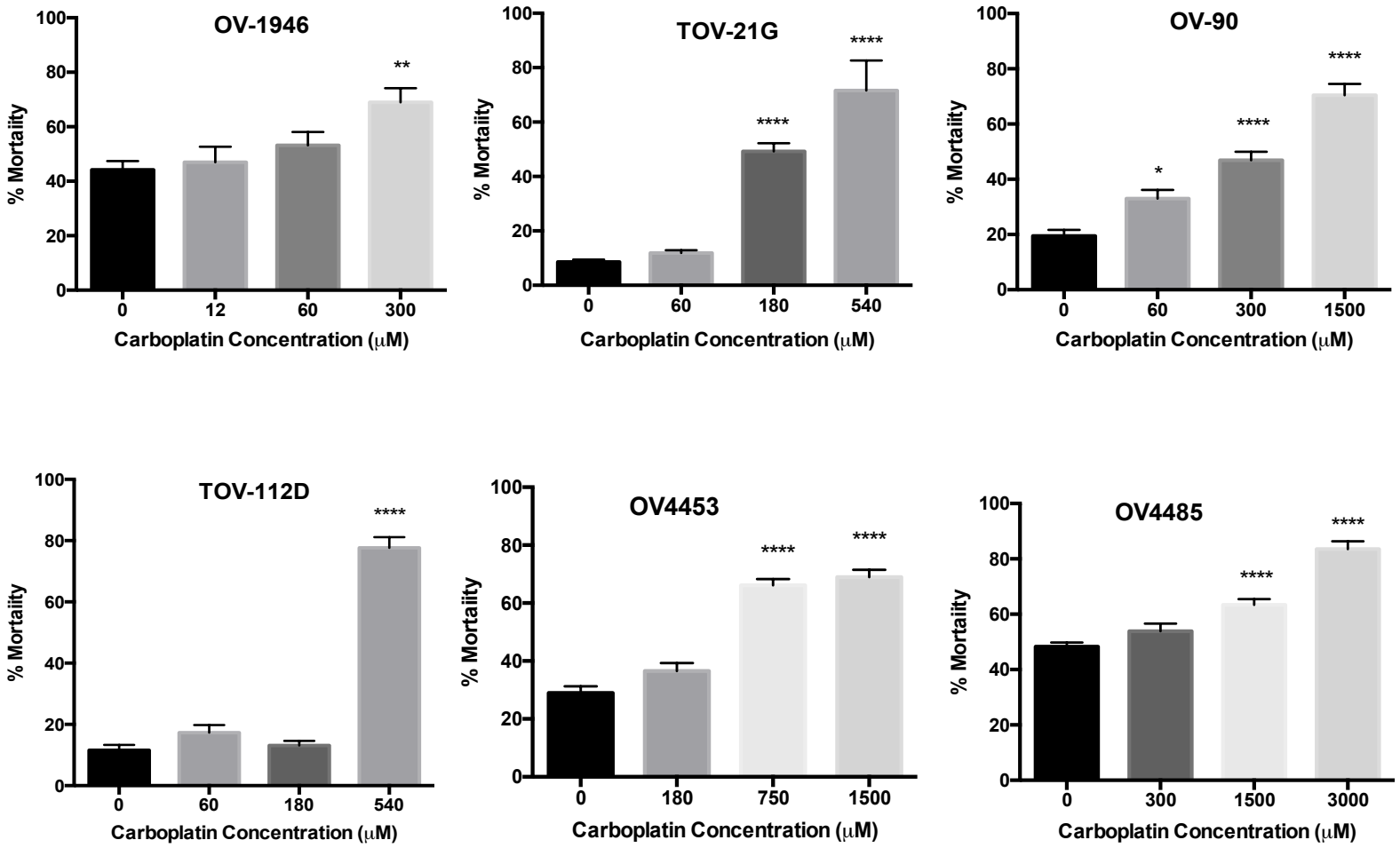

Figure S 2. **Carboplatin chemosensitivity in 3D spheroid models for all 6 EOC cell lines**

A) Absolute spheroid cell viability after three different carboplatin doses (24-hour treatments) B) Absolute spheroid cell mortality after three different carboplatin doses (24-hour treatments). All experiments were performed at least three times (range, 3-6). Error bar= ± SEM. *p<0.05, **p<0.01, ***p<0.001, ****p<0.0001